GEOPERSIA

Accepted Manuscript

Characterization of organic matter and petroleum generation potential of the Middle Jurassic Kashafrud Formation, Eastern Koppeh-Dagh, NE Iran: Implications for improved petroleum system understanding

Ali Shekarifard, Majid Safaei-Farouji, Elham Tarhandeh, Mehdi Namjoyan, Mehrab Rashidi, Hossein Bahrami

DOI: 10.22059/GEOPE.2025.389440.648800

Receive Date: 26 January 2025
Revise Date: 06 April 2025
Accept Date: 28 April 2025

Characterization of organic matter and petroleum generation potential of the Middle Jurassic Kashafrud Formation, Eastern Koppeh-Dagh, NE Iran: Implications for improved petroleum system understanding

Ali Shekarifard [1], *, Majid Safaei-Farouji [2] , Elham Tarhandeh [3], Mehdi Namjoyan [4], Mehrab Rashidi [3], Hossein Bahrami [3]

[1] Institute of Petroleum Engineering (IPE), School of Chemical Engineering, College of Engineering, University of Tehran, Tehran, Iran
[2] PhD Candidate, Department of Geosciences, University of Montanuniversität Leoben, Leoben, Austria
[3] Geochemistry Department Experts و Exploration Directorate, National Iranian Oil Company (NIOC), Tehran, Iran
[4] CEO of Petro Gostar Permayon Company, Tehran, Iran

Received: 26 January 2025, Revised: 06 April 2025, Accepted: 28 April 2025

Abstract
Geochemical characterization of organic matter (OM) from the Middle Jurassic Kashafrud Formation, as main possible source rock of the gas-fields in the Eastern Koppeh-Dagh from NE Iran, is main aim of this study. Rock-Eval VI pyrolysis, organic petrography, vitrinite reflectance (VRo), palynofacies, and molecular geochemistry analyses were performed on dark and black fine-grained siliciclastic and carbonate-siliciclastic sediments of the Formation from 5 wells and 10 outcrop sections. The total organic carbon (TOC) ranges from 0.10 to 1.37 wt% (on average: 0.46 wt%) and 0.04 to 1.5 wt% (on average: 0.56 wt%) for the surface sections and wells, respectively. Although mean residual TOC from the Kashafrud Formation is poor to fair but there are still good source rocks in the Formation that show higher content of carbonate with the higher TOC (up to 1.5 wt%). TOC and carbonate content show covariance. VRo ranges from 0,6 to 1,97% hence the kashafrud Formation is thermally early mature to over-mature. Kerogen is dominated by amorphoud organic matter (AOM) of phytoplanktonic origin with moderate to high amount of phytoclasts. Biomarker data confirms this result. The source rocks from the Kashafrud Formation, after maturing, generating, and expelling petroleum (gas and oil), can still be considered as a gas-prone source rock with Type III kerogen. Rock-Eval pyrolysis and organic petrography indicate presence of non-indigenous hydrocarbons (HCs) and therefore, confirm generation and expulsion of oil within the Kashafrud Formation. The mixed siliciclastic-carbonate facies, has played a more significant role in oil generation and expulsion. In the eastern Koppeh Dagh, there is still a chance of developing gas and even oil fields in potentual resrevoir rocks within the Kashafrud Formation and overlying formations.

Keywords: Organic Geochemistry, Organic Petrography, Middle Jurassic Kashafrud Formation, Eastern Koppeh-Dagh, NE Iran.

Introduction

The Amu-Darya basin is a petroliferous region in Turkmenistan and Uzbekistan, spreading towards Iran and Afghanistan. The basin contains a unique comprehensive petroleum system.

* Corresponding author e-mail: ashekary@ut.ac.ir

The bulk of the gas is located in Upper Jurassic carbonates and Neocomian clastics. Other stratigraphic intervals, from the Middle Jurassic to the Paleogene, have very few reserves. In the east-central part of the region, Lower to Middle Jurassic clastics and coal as well as Oxfordian black shales are responsible for gas generation. Source rock units are currently mature and, in the gas-window (Ulmishek, 2004).

The southwest part of the basin is in NE Iran, known as Koppeh-Dagh (Fig. 1). The Koppeh-Dagh was created after the Middle Triassic orogeny. It began to sink along the main faults. In its western and central parts, four principal active basement faults have been detected. In the eastern part of the basin, sedimentation was less or more continuous during the Middle Jurassic–Oligocene (Ulmishek, 2004).

The Khangiran gas-field (about 13 TCF) and two much smaller fields were discovered in the Koppeh-Dagh. The gas-fields are located in the folded rock layers in the Koppeh-Dagh. The Khangiran gas-field has resources in Neocomian clastic and Upper Jurassic carbonates; other fields are reservoired in Neocomian clastic. Despite extensive exploration and presence of many anticline, no fields have been discovered in other parts of the foredeep (Ulmishek, 2004). Accordingly, improved understanding of the petroleum system is vital.

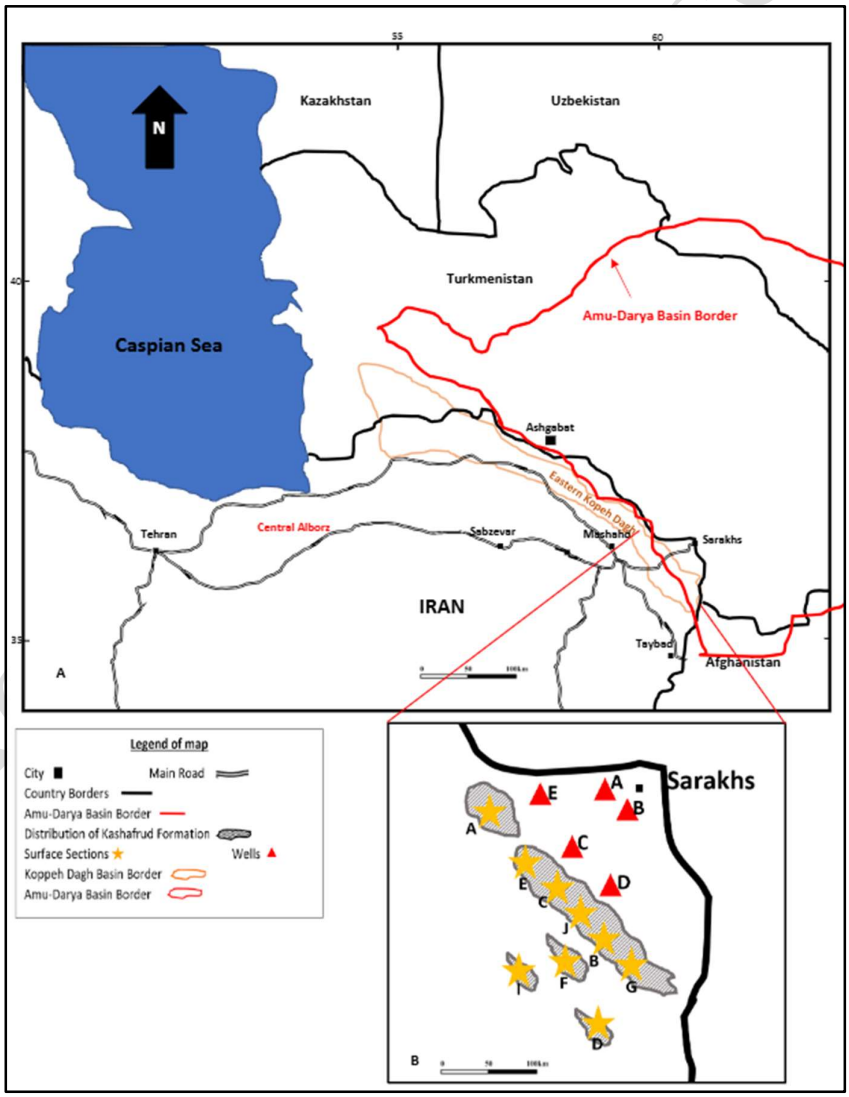

Figure 1. Study area and location of investigated surface sections and wells with distribution of Kashafrud Formation in NE Iran

Athough few study has been done on the petroleum generation potential of the Kashafrud Formation (Karamati et al., 2000; Zaheri, 2022), however the main challenging subjects for exploration is the insufficient knowledge on the possible source rock(s). Although the shaly sediments of the Kashafrud Formation are thought as principal and most important gas source rocks (Poursoltani & Gibling, 2011), however, so far, comprehensive organic geochemical investigation has not been done on them and are geochemically poorly understood. Furthermore, in NE Iran, other possible source rocks, such as the Callovian ChamanBid Formation, are known and need to be carefully investigated. This study is a comprehensive and complementary geochemical study on the dispersed organic matter (OM) from the shaly (organic-rich) facies of the Kashafrud Formation. To characterize the OM, techniques including Rock-Eval VI pyrolysis, palynofacies, organic petrography, vitrinite reflectance (Vro), gas-chromatography (GC) and gas chromatography-mass spectrometry (GC-MS) analyses were used. Because only the upper part of the Formation has been drilled, the presented results caracterize only the upper 200-500 meters of the Formation. Samples from the outcrops represent its entire thickness.

Geological setting and stratigraphy

During the Middle to Late Triassic, the subduction of the Iran Plate under the Turan Plate resulted in the closure of the Paleo-Tethys Ocean (Berberian and King, 1981; Wilmsen et al., 2009; Seifert et al., 2014). The Koppeh-Dagh was formed as a result of a back-arc extensional setting on the margin of Amu-Darya basin and Turan Plate (Fig. 1) (Garzanti & Gaetani, 2002; Brunet et al., 2003; Kazmin & Tikhonova, 2005). This extensional and highly subsiding depositional environment formed a thick sedimentary deposits during the Middle Jurassic and the Pliocene (Robert et al., 2014; Aghababaei et al., 2024).

During the Late Bajocian–Late Bathonian, maximum subsidence rates resulted in the deposition of the Kashafrud Formation in the eastern part of the Koppeh-Dagh (Moussavi-Harami & Brenner, 1992; Poursoltani et al., 2007). Additionally, the Kashafrud Formation may be extremely thick or completely absent above crest blocks or paleohighs. The Kashafrud Formation is predominantly conglomeratic at the base and is composed of siltstone, sandstone, and shale (Kavoosi et al., 2009).

The siliciclastic Kashafrud Formation with thickness of more than 2000m is outcropped along the southern boundary of Koppeh-Dagh. It rests heterogeneously and with angular unconformity on older rocks. It shows different depositional settings ranging from non-marine to marine enviroment. The dark and black thick shale from the uppermost part of the succession was deposited in a deeper marine setting (Taheri et al., 2009). In the study are, the Kashafrud Formation is gradually followed by the Callovian ChamanBid Formation – a unit composed of marl and argillaceous limestones – and, in some areas, by the Upper Jurassic Mozduran Formation (Fig. 2) (Taheri et al., 2009).

Constant deposition was formed until the upper Cretaceous, in which a general hiatus distinguished the border between Turonian and Maastrichtian throughout the Koppeh-Dagh. The primary inversion phase recorder in the Koppeh-Dagh happened in the Late Eocene (Frizon de Lamotte et al., 2011) and led to the folding of marine deposits up to the Late Eocene in the Alpine phase (Robert et al., 2014). Ultimately, the tectonic rearrangement in North Iran, which commenced in the Pliocene, resulted in the privilege of the strike-slip component in the present-day deformation of the Koppeh-Dagh (Robert et al., 2014).

During the Callovian, a marine transgression from the northwest of the Koppeh-Dagh caused the deposition of Mozduran carbonates. To the west of the Mozduran Formation, the ChamanBid Formation, deeper facies of Bathonian to early Oxfordian age, conformably overlies it (Lasemi, 1995).

The Shurijeh Formation records the continuation of fluvial deposition throughout the Neocomian (Moussavi-Harami, 1986). This Formation covers the Mozduran Formation, while is underlined by the Tirgan Formation. In the Eastern Koppeh-Dagh, the Mozduran and Shurijeh formations are main reservoirs for the gas-fields in NE Iran. To the northwest, the Shurijeh Formation gradually diminishes in thickness until it is totally supplanted by the Zard Formation, which is composed primarily of marine marls and calcareous shale with occasional sandstone beds (Afshar-Harb, 1979) (Fig. 2).

The Late Barremian-Early Aptian Tirgan Formation is composed of carbonate strata with subordinate siliciclastic interbeds. It conformably covers the red beds from the Neocomian Shurijeh Formation and underlined by the marl-shale beds from the Upper Aptian Sarcheshmeh Formation (Abad, 2017; Javanbakht et al., 2018).

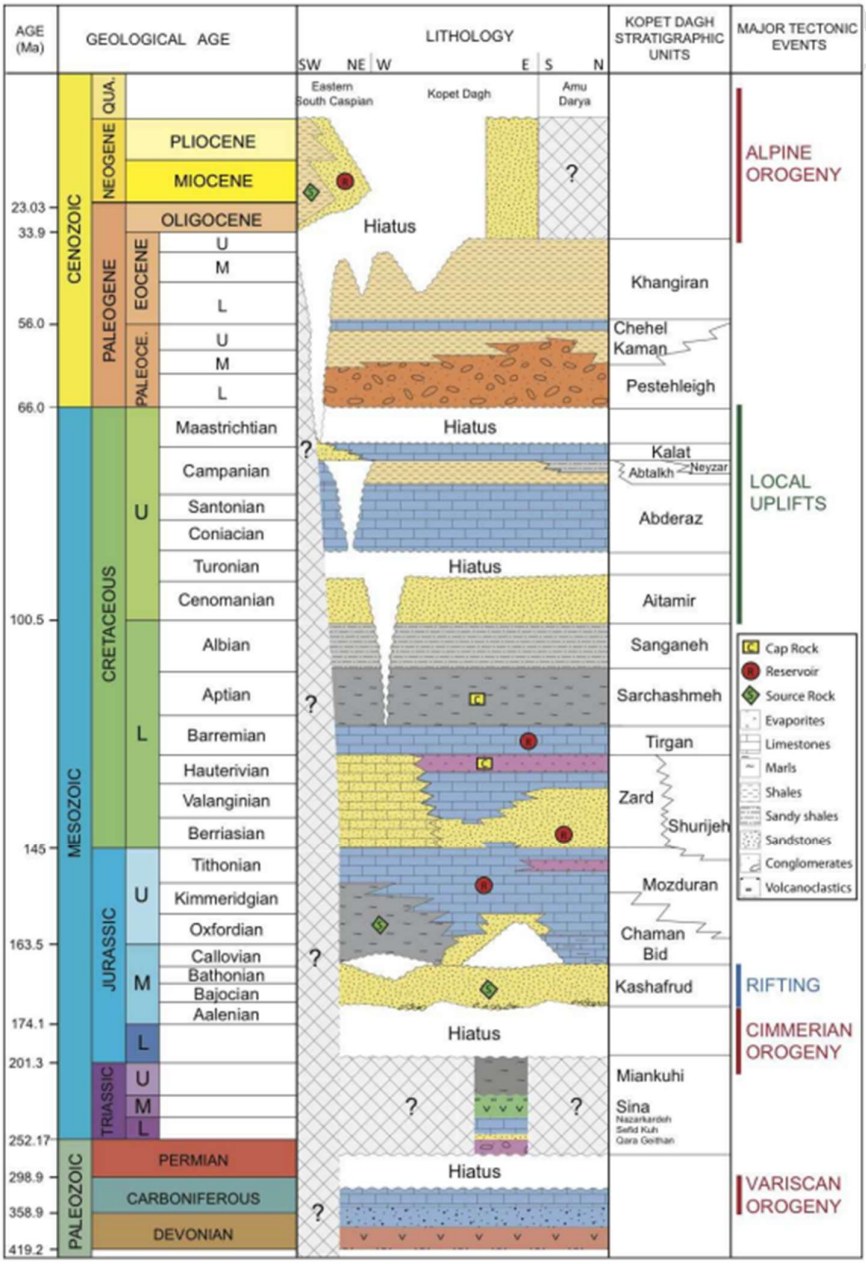

Figure 2. The stratigraphic chart of the Koppeh-Dagh basin and the setting of the Kashafrud Formation (Robert et al., 2014)

The Barremian-Aptian Sarcheshmeh Formation is composed of the lower 'marl member' and upper 'shale member' (Afshar-Harb, 1979). The Sarcheshmeh Formation with the age of is underlined by Sanganeh Formation.

The Albian Sanganeh Formation is composed of dark grey to black shale (Raisossadat & Moussavi-Harami, 1993) . The Late Albian to Cenomanian Aitamir Formation is composed of mudstone that graduates upward to a lower glauconitic sandstone, and finally to a unit of mudstone intercalated with sandstone (Sharafi et al., 2012). The Late Santonian Abderaz Formation is composed of calcareous and marly shales that lie beneath the mentioned erosional surface (Allameh et al., 2010). In the eastern Koppeh Dagh, the Campanian Abtalkh Formation is well evolved and has a lithology of calcareous shales (Afshar-Harb, 1979).

The Upper Campanian to Maastrichtian Kalat Formation is composed of limestone and carbonate build-ups (Afshar-Harb, 1979; Shahidi, 2008; Robert et al., 2014). The upper portion of the Kalat Formation is defined by an erosional surface that corresponds to the region's second general pause of sedimentation (Robert et al., 2014)

The Paleocene Pestehleigh Formation is characterized by a red continental series composed of sandstones and siltstones, followed by fluviodeltaic sediments. The upper Paleocene was determined in the white carbonate-bearing Chehel Kaman Formation. The transition to the Lower Eocene is marked by the presence of marl layers. The Eocene is characterized by varying limestones and marls, with the upper section becoming sandier (Robert et al., 2014).

The Early Eocene to Late Oligocene Khangiran Formation is composed of an intercalated succession of olive-gray calcareous shales (Afshar-Harb, 1969). It is generally underlain by the Chehel Kaman Formation, however because of the formation's sandwiching location inside the syncline, the top boundary is not evident (Moshirfar et al., 2015) (Fig. 2).

Sampling

In this study, 479 dark to black fine-grained siliciclastic and carbonatic-siliciclastic samples were collected from outcrops and wells. 440 samples come from 10 geological sections (outcrop sections A to J). The remaining 39 samples are cuttings from 5 wells (wells A to E) (Figure 1). Figure 2 shows the lithostratigraphy of the Kashafrud Formation in the studied outcrop sections and the position of samples collected. The well E covers the entire Kashafrud Formation, samples from the other wells represent only the upper 200 meters of the formation. Core samples from 3 meter deep wells were taken from outcrop sections J, E, and C, and their kerogen was extracted and investigated by Rock-Eval pyrolysis. To describe the general characterization of the Kashafrud Formation in the studied sections, some selected sections are following summarized.

In this part, sections D, E and G along with their sampling locations and lithological descriptions are discussed.

Section D (Fig. 3) is located in the Kashafrud River's northern reaches, 7 kilometers west of outcrop F. The actual thickness of the Kashafrud Formation in section D is 1215m. In section D, the Kashafrud Formation is overlain by the Sina Formation and progressive conglomerates with an angular unconformity. The Kashafrud Formation is composed of black to gray shale sequences (in some sequences with concretion) and sandstone layers containing sedimentary structures and plant fragments. Rarely do conglomerate lenses propagate in sandstone sequences. In this section, the Kashafrud Formation is underlain by the Mozduran Formation

Section E (Fig. 3) the real thickness of the Kashafrud Formation in section E is 678m. The Kashafrud Formation in this section is located in Paleozoic sequences with progressive microconglomerates. Sandstone and shaly layers cover this conglomerate sequence. Also, debris, in some cases, covers the shale layers. In the lower part of this section, a sequence of fossiliferous calcareous layers and argillaceous shales can be observed. In section E, the

Kashafrud Formation is conformably underlined by the Mozduran Formation.

Section G (Fig. 3) is located in the northern part of the Kashafrud river. The thickness of the Kashafrud Formation in this section is roughly 215m. In this section, the Kashafrud Formation covers Paleozoic strata with an angular unconformity. In the shaly part of section G, sandstone layers are widespread. Indeed, in this section, the Kashafrud Formation is mostly composed of conglomerate. Also, in the upper part, there is an unconformity between the Kashafrud Formation and the Mozduran Formation.

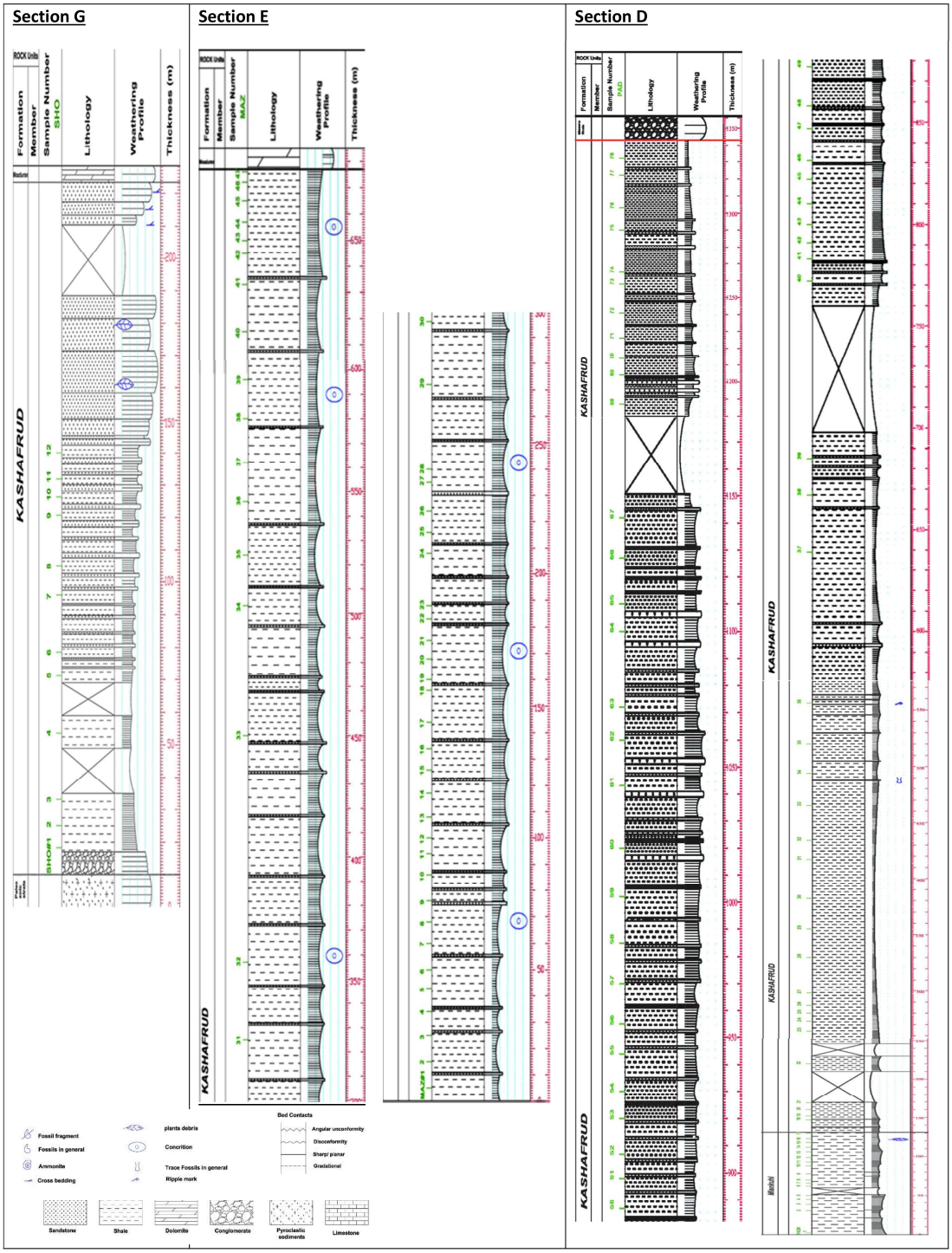

Figure 3. Lithostratigraphic columns of the some studied surface sections with sampling location

Analytical methods and results

Rock-Eval pyrolysis

The Rock-Eval VI pyrolysis analysis was performed on all samples. The prepared samples were heated to 600 °C at a rate of 25 °C /min in the presence of inert helium gas, employing a Rock-Eval VI™ instrument. After pyrolysis, the samples were transferred to an oven and were heated to 850 °C at a rate of 25 °C/min in the presence of high purity air. The Rock-Eval pyrolysis reults are listed in Table 1.

LECO analysis and carbonate measurement

The LECO CS-230 instrument was implemented to determine the organic carbon content of 8 selected samples and compare the measured values with TOC from the Rock-Eval pyrolysis. In this instrument samples are combusted at 1200 °C. In order to remove the carbonates, samples were first treated with hydrochloric acid (HF) 10%. In this case, the amount of carbon recorded in the device is wholly related to organic carbon.

To determine carbonate minerals content (calcite and dolomite), some samples selected and the carbonate bomb technique was used. In this experiment 5 cc of hydrochloric acid (HCl) 10% is added to one gram of sample powder. The carbonates react with the acid, and the pressure of the emitted CO_2 gas is related to the abundance of carbonate minerals. Table 2 shows the results of calcimetry for the selected samples.

Palynofacies analysis

In this part of study, 80 samples with a high TOC content and (HI) were selected for kerogen concentration. Roughly 100 grams of sample were crushed to a size of a few millimeters. Then 50% HCl and 33% HF was used, respectively (Green, 2001). Then slides were prepared and studied via the transmitted light LV 100 POL Nikon microscope.

Table 1. Rock-Eval VI pyrolysis parameters for well and outcrop samples from the Kashafrud Formation in NE Iran

Well/Outcrop	S_1			S_2			S_1+S_2 (PI)			T_{max}			S_3			TOC			HI			OI			S_2/S_3			S_1/TOC		
	Min	Max	Mean	Min	Max	Mean	Min	Max	Mean	Min	Max	Mean	Min	Max	Mean	Min	Max	Mean	Min	Max	Mean	Min	Max	Mean	Min	Max	Mean	Min	Max	Mean
WELL A	0.24	0.91	0.44	0.15	0.79	0.36	0.5	0.67	0.57	301	490	381	0.19	1.9	0.78	0.12	0.74	0.38	44	167	101	56	339	191	0.27	3.11	0.61	0.70	2.67	1.45
WELL B	0.91	1.86	1.39	0.32	0.96	0.64	0.62	0.83	0.68	361	445	399	0.08	0.34	0.18	0.22	0.59	0.40	138	325	160	22	250	47	1.85	8.6	4.21	2.46	7	3.74
WELL C	0.11	0.31	0.15	0.06	0.3	0.15	0.37	0.65	0.51	324	479	368	0.06	0.66	0.09	0.04	0.57	0.07	125	325	225	100	250	152	0.6	2.25	1.60	1.37	3.25	2.38
WELL D	0.2	1.07	0.71	0.3	1.69	1.25	0.29	0.46	0.36	313	450	374	0.66	3.63	2.50	0.57	1.5	1.21	53	113	99	116	242	196	0.45	0.86	0.50	0.35	0.78	0.57
WELL E	0.13	2.1	0.48	0.31	0.93	0.54	0.25	0.69	0.37	303	470	437	0.39	1.61	0.69	0.56	0.96	0.72	54	97	73	70	168	92	0.57	1.02	0.83	0.23	2.18	0.58
OUTCROP A	0	0.04	0.01	0	0.33	0.04	0	1	0.41	411	605	551	0.12	0.67	0.3	0.01	0.82	0.41	0	400	24	19	820	183	0	1.58	0.16	0	0.66	0.03
OUTCROP B	0	0.17	0.01	0	0.71	0.12	0	0.21	0.07	449	533	498	0.09	0.87	0.44	0.22	0.76	0.47	0	97	20	13	235	102	0	7.33	0.60	0	0.22	0.02
OUTCROP C	0	0.06	0.01	0	0.59	0.16	0	0.15	0.06	445	538	488	0.18	0.61	0.34	0.02	1.24	0.51	0	500	38	34	225	110	0	1.66	0.49	0	0.07	0.02
OUTCROP D	0	0.13	0.03	0	1.28	0.26	0	0.97	0.09	442	521	488	0.13	0.62	0.34	0.18	1.37	0.57	0	93	35	20	200	74	0	4.74	1.08	0	1.33	0.05
OUTCROP E	0	0.05	0.01	0	0.41	0.13	0	0.97	0.17	445	541	487	0	0.75	0.39	0	0.75	0.39	0	65	24	0	460	84	0	0	0	0	0	0
OUTCROP F	0	0	0	0	0.08	0	0	1	0.42	443	544	516	0	0.43	0.14	0	0.3	0.08	0	27	0.4	0	460	144	0	0	0	0	0	0
OUTCROP G	0	0.05	0	0	0.1	0.03	0.03	1	0.30	444	544	507	0	0.48	0.14	0	0.36	0.13	0	28	8	0	148	43	0	0	0	0	0	0
OUTCROP H	0	0.02	0	0	0.09	0.02	0.06	1	0.42	345	595	533	0.02	0.76	0.29	0	2	0.42	0	17	4	20	350	109	0	0.5	0.08	0	0	0
OUTCROP I	0	0.05	0.00	0	0.33	0.05	0	0.91	0.15	342	540	499	0.2	0.8	0.47	0.17	0.69	0.45	0	63	10	38	239	110	0	0.75	0.12	0	0.08	0.01
OUTCROP J	0	0.24	0.01	0	0.5	0.04	0	1	0.38	325	605	509	0.07	0.49	0.30	0.15	0.72	0.43	0	48	8	13	200	78	0	1.16	0.13	0	0.51	0.03

Table 2. The results of calcimetry of the selected samples from the Kashafrud Formation

Sample ID (depth from the base)	Outcrop	Total Organic Carbon (%)	Dolomite (%)	Calcite (%)	Total Carbonate (%)
GHS-1 (200m)	J	0.85	11	21	32
GHS-2 (290m)	J	0.63	13	39	52
GHS-3 (500m)	J	1.09	14	20	34
MAZ-1 (50m)	E	0.34	6	16	22
MAZ-2 (220m)	E	0.55	6	11	19
MAZ-3 (270m)	E	0.42	8	10	18
POL-1 (400m)	C	0.59	14	24	38
POL-2 (700m)	C	0.76	18	20	38

Kerogen petrography and vitrinite reflectance measurements

Vitrinite reflectance measurements were performed on 35 (27 from outcrops, 6 cuttings, and 2 shallow cores). Samples were crushed and mounted in a slow-setting resin. Once hardened, the blocks were polished using isopropyl alcohol as lubricant, initially using silicon carbide papers of successive finer grades of 320, 800 and 1200. This was then followed by different grades of alumina of initially 1 μm, then 0.3 μm and finally 0.05 μm. Kerogen petrography examination using Leica DM6000 microscope was carried out principally under oil immersion in reflected white light and UV light excitation.

It should be mentioned that for some study samples, two ranges of VRo (low and high range) were obtained. Low range of VRo is the indigenous values, slightly bitumen-impregnated and high VRo values could be attributed to oxidation effect which is indicated by reddish staining of the associated rock cuttings and therefore considered non-indigenous VRo values. The standard deviation of these samples (high VRo values) is rather high that is in the range of 0.16 to 0.48. The measured values of

Bitumen extraction and fractionation

Bitumen was extracted from approximately 30g of powdered sample, was kept in the Soxhlet instrument for 72 hours using a mixture of dichloromethane and methanol (93:7). The extracted bitumen was separated into saturated and aromatic HCs as well as NSO compounds fractions by liquid column chromatography. A 300.72 cm chromatographic column was packed with 60–120 mesh silica gel, activated for 2 hours at 120 °C, and capped with a few cm of alumina. The column was then developed with solvents of increasing polarity, i.e., light petroleum (100 ml), dichloromethane (100 ml) and methanol (50 ml). The fractions were collected in separate 250 ml round-bottom flasks. The solvent was later reduced by the Buchi evaporation instrument, and the weights of the fractions were recorded.

Gas-Chromatography (GC) and Gas Chromatography-Mass Spectrometry (GC-MS) analysis

For GC and GC-MS analysis 47 samples (17 cuttings and 27 outcrops) were selected for analyzing the molecular geochemistry properties of bitumen. Results are listed in Tables 4 and 5. Prior to chromatographic analysis, silica, alumina, and cotton wool were Soxhlet pre-extracted in dichloromethane (DCM) for 48 hours, followed by drying at nearly 30°C. The extracted silica and alumina were kept activated in an oven at 110°C until required. A chromatographic column (30×0.72 cm) was packed with silica gel of 60–120 mesh and capped with a few cm of alumina. The column was then developed with solvents of increasing polarity, i.e., light petroleum (100 ml), dichloromethane (100 ml) and methanol (50 ml). The eluates were collected in separate 250 ml round-bottom flasks. The solvent was also reduced by Buchi evaporation, and the weights of the eluates were recorded. The saturate and aromatic hydrocarbon (HC) fractions were analyzed by GC and GC-MS. The GC analysis was conducted employing an Agilent 5975B column (50m, 0.32mm i.d.). The temperature was programmed to range between 40 and 300 °C at a rate of 4 °C/min. It was then kept at 300 °C for 30 minutes. The saturated and aromatic fractions were then analyzed by an Agilent 5975B inert MSD mass spectrometer with a gas chromatograph attached directly to the ion source. The measured values for some of investigated samples were summarized in Tables 4, 5 & 6.

Isotopic analysis

This analysis was conducted using Finnigan MAT delta S type stable isotope ratio mass spectrometer.

Table 3. Vitrinite reflectance (VRo) measurement results on the selected samples from the Kashafrud Formation

Sample. No	Sample Type	Sample ID	Well/Outcrop	Min	Max	Mean	Readings	Std Dev
1	Cuttings	KG 30 – K1	A	0.8	0.99	0.9	6	0.09
2		KG 16 – 2	B	0.86	1.1	0.96	18	0.09
3		AA 1 – 1	C	0.99	1.2	1.12	8	0.08
4		TS 1– 2	D	0.93	1.3	1.12	25	0.09
5		ATR 1 – 1	E	0.91	1.13	1.01	32	0.06
6		ATR 1 – 4	E	0.9	1.2	1.09	25	0.09
7	Core	KG 30 – K1	A	1.66	2.04	1.89	25	0.11
8		AA 1 – K	C	1.6	1.96	1.78	25	0.09
9	Outcrops	AGH-1	OUTCROP F	0.65	0.85	0.75	20	0
10		GHGH-3	OUTCROP B	0.6	0.91	0.69	25	0.07
11		GHGH-13	OUTCROP B	0.5	0.78	0.6	25	0.08
12		PAD-4	OUTCROP D	1.04	1.21	1.11	13	0.05
13		PAD-16	OUTCROP D	1.07	1.31	1.19	4	0.09
14		PAD-19	OUTCROP D	1.19	1.58	1.36	7	0.13
15		PAD-75	OUTCROP D	1.2	1.6	1.46	8	0.14
16		MAZ-14	OUTCROP E	0.71	0.98	0.88	15	0.09
17		MAZ-40	OUTCROP E	0.7	0.9	0.8	15	0.07
18		MAZ-44	OUTCROP E	0.67	0.91	0.79	25	0.07
19		KAR-10	OUTCROP I	0.97	1.24	1.11	25	0.08
20		KAR-33	OUTCROP I	0.83	1.16	0.94	25	0.09
21		KAR-56	OUTCROP I	0.78	1.18	0.89	25	0.09
22		MIMY-25	OUTCROP A	1	1.25	1.15	7	0.09
23		MIMY-82	OUTCROP A	1.4	1.69	1.54	14	0.09
24		MIMY-107	OUTCROP A	0.85	1.23	1.05	20	0.11
25		KOL-36	OUTCROP H	1.28	1.59	1.44	25	0.08
26		KOL-51	OUTCROP H	0.99	1.21	1.11	11	0.08
27		KOL-63	OUTCROP H	1.24	1.49	1.34	25	0.07
28		KOL-107	OUTCROP H	0.76	0.99	0.88	25	0.06
29		GHS-16	OUTCROP J	0.83	1.11	0.95	25	0.08
30		GHS-22	OUTCROP J	0.7	0.97	0.84	30	0.07
31		GHS-28	OUTCROP J	0.78	1.1	0.94	30	0.08
32		POL-16	OUTCROP C	0.83	1.09	0.95	25	0.07
33		POL-43	OUTCROP C	0.83	1.14	1	25	0.09
34		POL-63	OUTCROP C	0.64	0.87	0.77	25	0.07
35		SHO-5	OUTCROP G	0.57	0.75	0.66	25	0.06

Firstly, the sample was oxidized by copper oxide (CuO) in Pyrex tubes to 480 °C (Sofer, 1980). Then, after vacuum distillation, the ratios of C^{13}/C^{12} were determined based on the CO2 evolution. The stable carbon isotope values are reported in the d format compared to V-PDB standard (Coplen, 1995), with the experimental accuracy predicted to be ±0.2‰. Results are listed in Table 7.

Discussion

Geochemistry and petrography of the source rock

TOC richness

The mean TOC content in (cutting) well samples (mostly from the upper 200 meters of the Formation) is 0.56 wt%, while it is 0.41 wt% in outcrop samples. The maxumum TOC is 1.5 wt% and 1.37 wt% for the cutting and outcrop samples, respectively.

Table 4. Gas chromatography (GC) and GC-mass spectrometry (MS) analysis results of the saturate fraction from the selected samples of the Kashafrud Formation

Well/Outcrop	Sample ID	Pr/Ph	Pr/nC$_{17}$	Ph/nC$_{18}$	CPI	Sterane/Hopane	C$_{26}$/C$_{25}$ Terpanes	C$_{31}$R/C$_{30}$ Hopane	C$_{29}$/C$_{30}$ Hopane	% C$_{27}$ Sterane	% C$_{28}$ Sterane	% C$_{29}$ Sterane	C$_{27}$ Dia./(Dia+Reg)	C$_{27}$/C$_{29}$ Steranes	C$_{23}$Tri/C$_{24}$Tri	Ts/Tm	C$_{31}$-hopane 22S/(22S+22R)	C$_{29}$-Sterane 20S/(20S+20R)
WELL A	KG 30-K1	0.73	0.36	0.45	1.01	--	0.71	0.33	1.5	--	--	--	--	--	1.89	1.00	0.6	--
WELL A	KG 30-K2	0.75	0.23	0.3	1.03	--	0.8	0.2	0.94	--	--	--	--	--	2.1	0.79	0.56	--
WELL C	AA 1-K	1.03	0.32	0.39	0.96	--	0.75	0.63	1	--	--	--	--	--	2.1	1.88	0.5	--
WELL B	KG 16-2	0.49	0.49	0.66	0.93	2	0.89	0.17	1.43	39.2	30.1	30.7	0.63	1.27	2.22	1.17	0.64	0.28
WELL C	AA 1-1	0.91	0.55	0.57	1.01	1.01	1	0.22	1.04	47.7	19.8	30.6	0.75	1.46	1.72	1.50	0.65	0.47
WELL D	TS 2	0.92	0.52	0.64	0.91	1.43	0.95	0.13	1.26	53.7	23.8	22.4	0.58	2.47	2.19	1.00	0.58	0.5
WELL E	ATR 1-1	1.25	0.48	0.48	1	1.33	1.1	0.21	0.93	51.9	18	30.1	0.57	1.73	2.03	1.56	0.61	0.58
WELL E	ATR 1-4	1.13	0.63	0.66	0.99	1	0.13	0.21	1.58	60.7	20.7	18.6	0.47	3.26	2.24	1.42	0.68	0.48
OUTCROP B	GHGH-3	0.85	0.54	0.58	0.96	2.78	1	0.29	1.5	42.5	30	27.5	0.75	1.5	2.5	2.00	0.57	0.46
OUTCROP B	GHGH-13	0.67	0.5	0.58	0.86	--	0.83	0.20	0.9	--	--	--	--	--	2.4	0.83	0.55	--
OUTCROP D	PAD-75	0.67	0.52	0.58	1.02	3.15	0.98	0.27	1.73	51.5	19.2	29.2	0.58	1.73	2.27	1.50	0.63	0.59
OUTCROP E	MAZ-40	1.89	0.55	0.3	1.02	--	1	0.3	1.4	--	--	--	--	--	2.66	0.75	0.55	--
OUTCROP E	MAZ-44	2.20	0.68	0.31	1	1.88	1	0.43	1.14	64.4	16.1	19.5	0.64	3.29	2.1	1.53	0.54	0.59
OUTCROP E	MAZ-44	2.20	0.68	0.31	1	1.23	1	0.23	1.08	66.3	16.3	17.4	0.58	3.8	2.3	1.15	0.54	0.59
OUTCROP I	KAR-10	0.87	0.57	0.63	0.95	--	0.86	0.25	1.1	--	--	--	--	--	2.56	1.60	0.5	--
OUTCROP I	KAR-33	0.81	0.77	0.93	0.93	--	0.67	0.67	1.67	---	--	--	--	--	2.13	1.17	0.55	--
OUTCROP I	KAR-56	0.73	0.56	0.63	0.88	--	0.5	0.33	1.67	---	--	--	--	--	2.17	1.67	0.5	--
OUTCROP A	MIMY-25	0.73	0.59	0.7	0.91	--	1	0.2	1.2	--	--	--	--	--	2.31	1.00	0.55	--
OUTCROP A	MIMY-82	0.81	0.52	0.6	0.92	--	0.75	0.36	1	--	--	--	--	--	3.06	1.75	0.54	--
OUTCROP A	MIMY-107	1.14	0.44	0.38	0.93	1	1.1	0.25	0.88	47.9	28.8	23.3	0.72	2.06	2.11	3.00	0.57	0.65
OUTCROP H	KOL-36	0.62	0.51	0.66	0.95	2.28	0.67	0.2	1.2	43.5	26.1	30.4	0.68	1.43	2.19	1.17	0.6	0.48
OUTCROP H	KOL-51	0.58	0.4	0.54	0.54	1.82	1.1	0.25	1	58.3	22.2	19.4	0.45	3	2.37	1.40	0.4	0.53
OUTCROP H	KOL-63	0.57	0.45	0.6	0.95	--	1	0.3	1.2	--	--	--	--	--	2.22	1.00	0.55	--
OUTCROP H	KOL-107	0.74	0.54	0.55	0.95	3.01	1.33	0.31	1.08	56.3	25.9	17.9	0.37	3.15	2.31	1.17	0.6	0.56
OUTCROP J	GHS-16	0.88	0.44	0.48	0.91	2.8	1	0.2	1.67	50	30	20	0.56	2.5	2.07	1.40	0.5	0.59
OUTCROP J	GHS-22	2.5	0.43	0.17	0.97	--	--	--	--	--	--	--	--	--	--	--	--	--
OUTCROP J	GHS-28	1.25	0.51	0.4	0.99	3.59	0.98	0.33	1.08	60.5	11.6	27.9	0.37	2.17	2.68	1.17	0.5	0.27
OUTCROP C	POL-16	1.23	0.36	0.27	0.96	--	0.98	0.2	1.4	--	--	--	--	--	2.11	1.67	0.5	--
OUTCROP C	POL-43	1	0.38	0.33	0.98	2.28	0.94	0.3	1.3	45.5	34	19.8	0.51	3.53	2.5	0.75	0.44	0.52
OUTCROP C	POL-63	1.37	0.48	0.53	0.98	--	2	0.32	1.17	--	--	--	--	--	3.93	0.22	0.63	--
OUTCROP G	SHO-5	0.83	0.58	0.66	0.93	1	1	0.27	1.34	61.8	23.6	14.5	0.75	4.25	2.22	0.33	0.66	0.61
OUTCROP F	AGH	0.75	0.27	0.34	1.04	2.19	0.75	0.26	1	39.2	21.6	39.2	0.5	1	2.1	0.86	0.56	0.46

Table 5. GC-MS analysis results of the aromatic fraction from the selected samples of the Kashafrud Formation

Well/Outcrop	Sample ID	MPI-1	MPI-2	4-MDBT/1MDBT	DBT/Phen	Remarks
WELL A	KG 30-K1	0.68	0.84	6.36	0.13	
WELL A	KG 30-K2	0.79	0.92	2.24	0.09	
WELL C	AA 1-K	0.71	0.83	4.83	0.29	
WELL B	KG 16-2	0.71	0.83	3.94	0.69	Non-indigenous HC
WELL C	AA 1-1	0.22	0.25	3.56	0.01	Indigenous HC
WELL D	TS 2	0.71	0.84	3.16	1.01	Non-indigenous HC
WELL E	ATR 1-1	0.89	0.98	5.6	0.25	Indigenous HC
WELL E	ATR 1-4	0.96	1.14	4	1.20	Non-indigenous HC
OUTCROP B	GHGH-3	0.47	0.6	4.34	0.04	
OUTCROP B	GHGH-13	0.5	0.57	3.56	0.07	
OUTCROP D	PAD-75	0.27	0.35	9.85	0.04	
OUTCROP E	MAZ-40	0.54	0.71	5.8	0.02	
OUTCROP E	MAZ-44	0.73	0.87	7.77	0.08	
OUTCROP E	MAZ-44	0.68	0.76	5.71	0.06	
OUTCROP I	KAR-10	0.75	0.94	7	0.02	
OUTCROP I	KAR-33	0.37	0.5	5.18	0.05	
OUTCROP I	KAR-56	0.54	0.72	5.38	0.04	
OUTCROP A	MIMY-25	0.31	0.34	4.83	0.15	
OUTCROP A	MIMY-82	0.44	0.5	3.78	0.06	
OUTCROP A	MIMY-107	0.42	0.54	4.96	0.04	
OUTCROP H	KOL-36	0.13	0.16	3.72	0.01	
OUTCROP H	KOL-51	0.44	0.74	12.45	0.01	
OUTCROP H	KOL-63	0.33	0.47	6.6	0.01	
OUTCROP H	KOL-107	0.23	0.28	2.74	0.01	
OUTCROP J	GHS-16	0.56	0.76	3.74	0.02	
OUTCROP J	GHS-22	0.91	1	4.68	0.04	
OUTCROP J	GHS-28	0.56	0.7	4.2	0.03	
OUTCROP C	POL-16	0.96	1.2	5.46	0.03	
OUTCROP C	POL-43	0.41	0.49	2.7	0.02	
OUTCROP C	POL-63	0.52	0.6	2.95	0.02	
OUTCROP G	SHO-5	0.39	0.52	3.59	0.01	
OUTCROP F	AGH	0.58	0.69	3.43	0.44	

In order to assess the reliability of the TOC, eight samples from outcrops B, C, and D were selected and analysed via LECO method. For the selected samples, the mean TOC contents measured by Rock-Eval and LECO analysis are 0.65 wt% and 0.75 wt%, respectively. For the samples there is a direct relationship between TOC values measured by LECO and Rock-Eval analysis (Fig. 4).

Table 6. The comparison of the GC and GC-MS results of indigenous and non-indigenous bitumens

Sample ID	Bitumen	Pr/Ph	Pr/nC_{17}	Ph/nc_{18}	CPI	DBT/Ph	Sterane / Hopane	C_{24}/C_{25} Terpanes	C_{29}/C_{30} Hopane	C_{27} Dia/ (Dia+Reg)	C_{29}/ C_{29} Steranes	Ts/Tm	C_{31}-hopane 22S/(22S+22R)	C_{29}-Sterane 20S/(20S+20R)	MPI-1	MPI-2	4-MDBT/1MDBT
ATR 1-1	iHC	1.25	0.48	0.48	1	0.25	1.33	1.1	0.93	0.57	1.73	1.56	0.61	0.58	0.89	0.98	5.6
AA 1-1	iHC	0.91	0.55	0.57	0.93	0.01	1.01	1	1.04	1.04	1.46	1.46	0.65	0.28	0.22	0.25	3.56
Mean	-	1.08	0.51	0.52	0.96	0.13	1.17	1.05	0.98	0.80	1.59	1.51	0.63	0.43	0.55	0.61	4.58
TS 2	non-iHC	0.92	0.52	0.64	1.01	1.01	1.43	0.95	1.26	1.26	2.47	2.47	0.58	0.47	0.71	0.84	3.16
ATR 1-4	non-iHC	1.13	0.63	0.66	0.99	0.99	1	0.13	1.58	0.47	3.26	1.42	0.68	0.48	0.96	1.14	4
KG 16-2	non-iHC	0.49	0.49	0.66	0.93	0.69	2	0.89	1.43	1.43	1.27	1.27	0.64	0.28	0.71	0.83	3.94
Mean	-	0.84	0.54	0.65	0.97	0.89	1.47	0.65	1.42	1.05	2.33	1.72	0.63	0.41	0.79	0.93	3.7

iHC: indigenous HC; non-iHC: non-indigenous HC

Table 7. Carbon isotope composition of saturate and aromatic fractions from the selected samples

Well/Outcrop	$\delta^{13}C$ Saturate (‰)	$\delta^{13}C$ Aromatic (‰)	Canonical variable (CV)
Well A	-28.1	-26.0	1.723
Well B	-27.3	-26.8	-2.077
Well D	-27.3	-25.5	0.809
Well E	-24.4	-24.6	-4.53
Well E	-27	-25.7	-0.394
Outcrop B	-27.3	-25.1	1.697
Outcrop C	-26.5	-24.5	1.005
Outcrop D	-25.7	-23.7	0.757

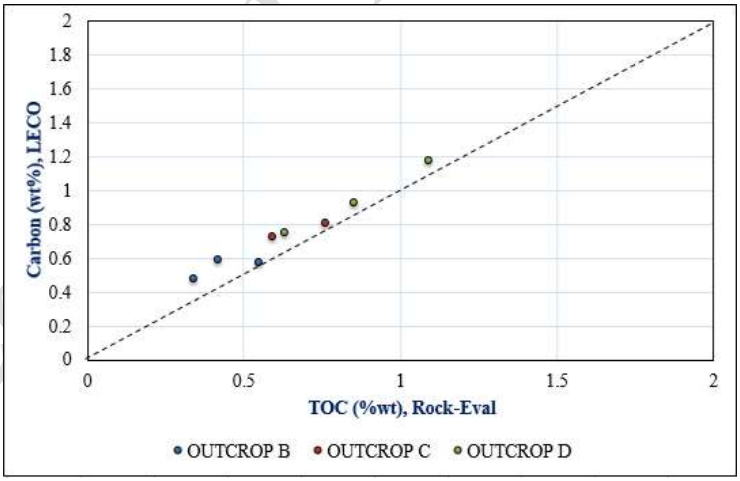

Figure 4. Comparison of total organic carbon (TOC) content obtained by Rock-Eval and LECO analysis

Dark and black samples from the outcrops and cuttings show more or less the same range and mean of TOC content. Based on the experienced level of maturation, undoubtedly, immature samples had a higher content of TOC. There is a general positive relationship between residual TOC and carbonate contents in these samples. Mean TOC for the section D is highest value (0.86 wt%) and mean carbonates content is maximum as well (39.3 wt%). This indicates with increasing the mean TOC, the mean carbonate content also increases (Fig. 5). In terms of petroleum generation and expulsion, compared to pure siliciclastic source rocks, the carbonate

source rocks have better potential to generate and expel oil (Hunt, 1996; Jones, 1984). Although mean residual TOC from the shay facies of the Kashafrud Formation is poor but there are still good source rocks in the Formation that show higher content of carbonate minerals with the higher organic matter.

Petroleum generation potential

Petroleum potential ($PP=S_1+S_2$) is a practical measure to evaluate the petroleum potential of a given source rock (Tissot and Welte, 1978). Due to the high level of maturation, the petroleum generation potential of the investigated samples is, in fact, residual potential. As depicted in Fig. 6a, only some samples from wells B and D have still fair petroleum potential (up to 3.01 mg HC/g rock) for generation, but other cuttings samples are poor to very poor potential. In spite of cuttings, all outcrop samples show very poor to poor residual PP and occasionally, this parameter (PP) reaches up to 1.38 mg HC/g rock. Correspondingly, cuttings, in general, denote higher mean residual PP (1.2 mg HC/g rock) than outcrop samples (0.08 mg HC/g rock) from the Kashafrud Formation (Fig. 6b). As discussed in section 5.1.5, some cutting samples are stained by the migrated HCs (samples with MI>150) and therefore, higher amounts of residual PP values are partly due to the presence of migrated HCs. Residual PP for the cuttings without the migrated HCs, ranging from 0.21 to 2.70 (on average: 1.15 mg HC/g rock).

In terms of petroleum generation potential, the samples from outcrops and cuttings have more or less the same potential, the result of maturation and oxidation of OM.

Origin and type of the Kerogen

Various methods are used to investigate kerogen in terms of its type, and origin. These techniques include elemental analysis (measuring hydrogen content), Rock-Eval pyrolysis, kerogen microscopic observations, and molecular geochemistry investigations (Tissot & Welte, 1984). Comparison of these methods while confirming the results can provide the required information about the origin and type of kerogen.

The hydrogen index (HI) is the first parameter that is employed to evaluate the type of kerogen. However, the current study results show that this parameter should be carefully evaluated, especially the samples with low TOC (less than 1 wt%).

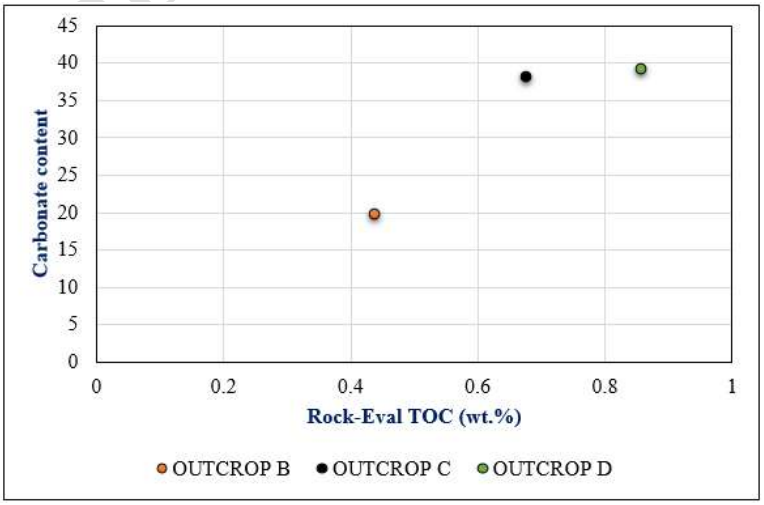

Figure 5. Cross plot of mean TOC content measured by Rock-Eval pyrolysis versus mean carbonate content obtained via calcimetry analysis

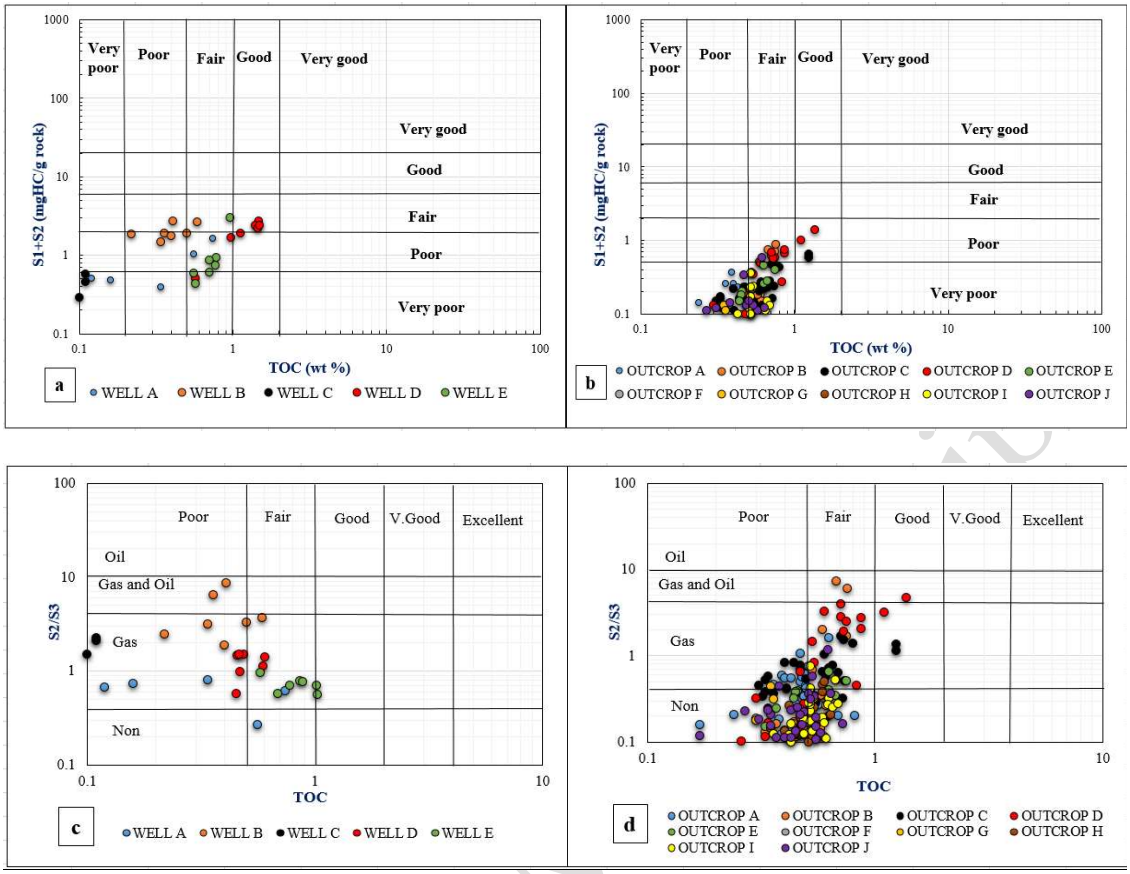

Figure 6. Cross plot of TOC against production index (S1+S2) illustrating hydrocarbon generation potential of well (a) and outcrop samples (b), the plot of S2/S3 ratio versus TOC (c & d) showing the type of generated hydrocarbon

Based on plots of S_2/S_3 versus TOC, almost all samples from the five wells are presently gas-prone (Type III Kerogen) (Fig. 6c), whereas, nearly all samples from outcrops E, F, G, H, I indicate the presence of Type IV kerogen (Fig. 6d). However, some samples from the rest of outcrops (A, B, C, and D) have gas-prone OM (Type III Kerogen). The same results are achieved based on the plot HI-Tmax for the same samples from the wells and surface sections (Figs 10 a & b). It should be noted that the samples with suitable value of S_2 (more than 0.2 mg HC/g rock) were selected and plotted on the diagrams (Peters, 1986).

The mean HI value for the cuttings and outcrop samples is 136 mg HC/g TOC and 46 mg HC/g TOC, respectively. Difference in HI values and the occurrence of Type IV kerogen in the outcrop samples could be the result of weathering and mineral-matrix effect. In general, the surface weathering and mineral-matrix effect reduce HI value and Type III kerogen is classified as samples with Type IV kerogen. In terms of petroleum generation potential of a basin, it is always important to distinguish Type IV kerogen from Type III. To solve the problem and evaluate the effect of weathering and mineral-matrix on the HI value for the outcrop samples, relatively-subsurface samples (3-meter cores) selected and their kerogen was isolated and investigated by Rock-Eval instrument.

For example, at sections B, C, and D, mean HI value for three shallow core samples is 43 mg HC/g TOC, and for kerogens isolated from the same samples is 80 mg HC/g TOC. This indicates the mineral-matrix has played an important role in lowering HI value.

Although kerogen extraction is performed to accurately evaluate the parameters of Rock-Eval pyrolysis, but for OM-lean samples, pure kerogen cannot always be obtained, and part of the matrix always remains in kerogen. Therefore, the calculated HI for kerogen samples in some

cases still does not show the actual value. In this stage thus, the HI values for rock samples were calculated and corrected based on the S_2-TOC diagram (Fig. 7). The regression line equation of the S_2-TOC diagram for core samples in sections B, C, and D (with mean HI value of 31 mg HC/g TOC) is Y = 1.271X-0.4947 and R^2 = 0.85 (Fig. 7). According to the HI = S_2/TOC equation, mean HI calculated for these samples is 127 mg HC/g TOC confirming the existence of Type III kerogen.

The arguments mentioned obviously represent a change in facies with predominantly Type IV kerogen to Type III kerogen-rich facies. This is a significant result demonstrating that at least some outcrop samples from the Kashafrud Formation, which show Type IV kerogen, have, in fact, Type III kerogen. Due to experiencing maturation, this amount of HI represents the residual HI, and therefore higher HI values existed in immature conditions.

In contrast to outcrop samples, some cutting samples show a slight overestimation in HI values due to the presence of non-indigenous/migrated HCs. For example, in well B, high PI value up to 0.68 and MI value of up to 450 obviously indicate the presence of non-indigenous or migrated HCs (Jarvie et al., 2001). Heavy compounds of non-indigenous HCs always appear at peak S_2. This property, along with low TOC cause an overestimation in HI value.

Furthermore, in well B, the HI value of one sample with very low TOC (0.22 wt%) is 145 mg HC/g TOC. In this sample, as a poor or non-source rock, the amount of S_1 is 1.54 mg HC/g rock, S_2 is 0.32 mg HC/g rock, PI is 0.83, and MI is 700. These parameters clearly represent the presence of migrated HCs. In this sample part of the S_2 value is very likely related to heavy migrated HCs because this low amount of TOC cannot show such S_2 peak. However, the mean HI value for the cutting samples without non- indigenous/ migrated HCs is 99 mg HC/g that still confirm the presence of Type III Kerogen.

In light of the foregoing interpretations, based on the Rock-Eval data, samples from some surface sections are primarily comparable to those of studied well samples. Currently, the Kashafrud Formation in most surface sections and wells (except for well C), after experiencing maturation, has primarily Type III kerogen.

Kerogen in the dark and black shale samples is derived from both continental and marine origin, including amorphous OM (AOM), phytoclasts, and palynomorphs. The palynofacies is characterized by dominance of AOM, with moderate to high contribution of phytoclasts and occurrence of palynomorphs (Figs 8 & 9).

The occurrence of marine palynomorphs indicate the shales from the Formation in some intervals have been experienced marine environments and therefore, some parts of AOM may have originated from marine organisms (Taheri et al., 2009) (Fig. 8). Accumulation and diagenesis of these materials led to the formation Type II and II/III kerogen in immature state.

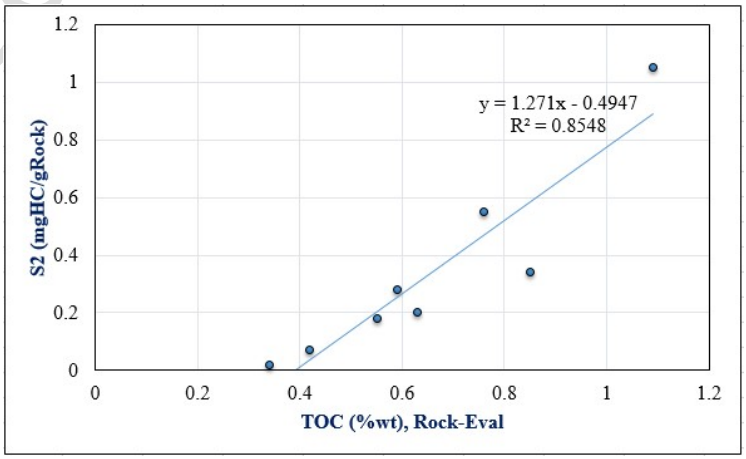

Figure 7. The plot of TOC versus S2 for core samples illustrating the mineral matrix effect

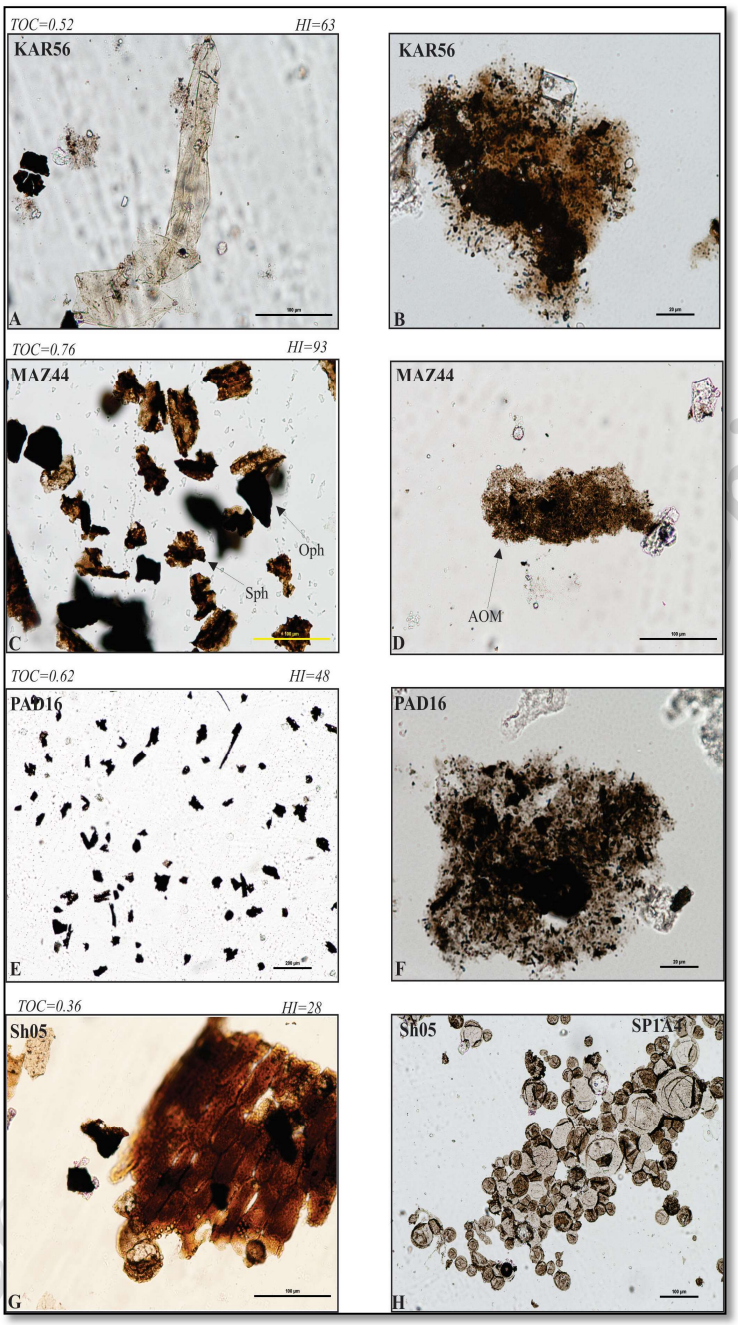

Figure 8. Microscopic images (under transmitted light) of dispersed organic matter in the shay sediments from the Kashafrud Formation. A and B: Transparent / membrane phytoclasts longer than 400 microns with semi-opaque phytoclasts on the left of the image and amorphous organic matter with dispersed particles with the possible origin of marine microorganisms in the same sample. C: opaque and semi-opaque phytoclasts (gelled and amorphous) with amorphous organic matter on the right part (D) of the same sample. E: opaque phytoclasts with amorphous materials on the right part (F) of the same sample. Note the absence of semi-opaque particles. G: Well-preserved cuticle with the cellular structure of epidermal tissue and algal spores on the right (H) of the same sample

In consistent with the palynofacies analysis, the molecular geochemistry results of bitumen, demonstrate main part of AOM has a marine origin and has derived from marine phytoplankton and algal, although terrestrial and continental origin cannot be fully ruled out. Therefore, it is

logic to assume AOM in the samples, especially from marine intervals, can be classified as oil-prone AOM (Type II or II/III kerogen). These materials in immature status, have good potential to generate a lot of petroleum during the advanced maturation. However, problem of liquid HCs expulsion for the samples with low TOC could be a case in the Kashafrud Formation.

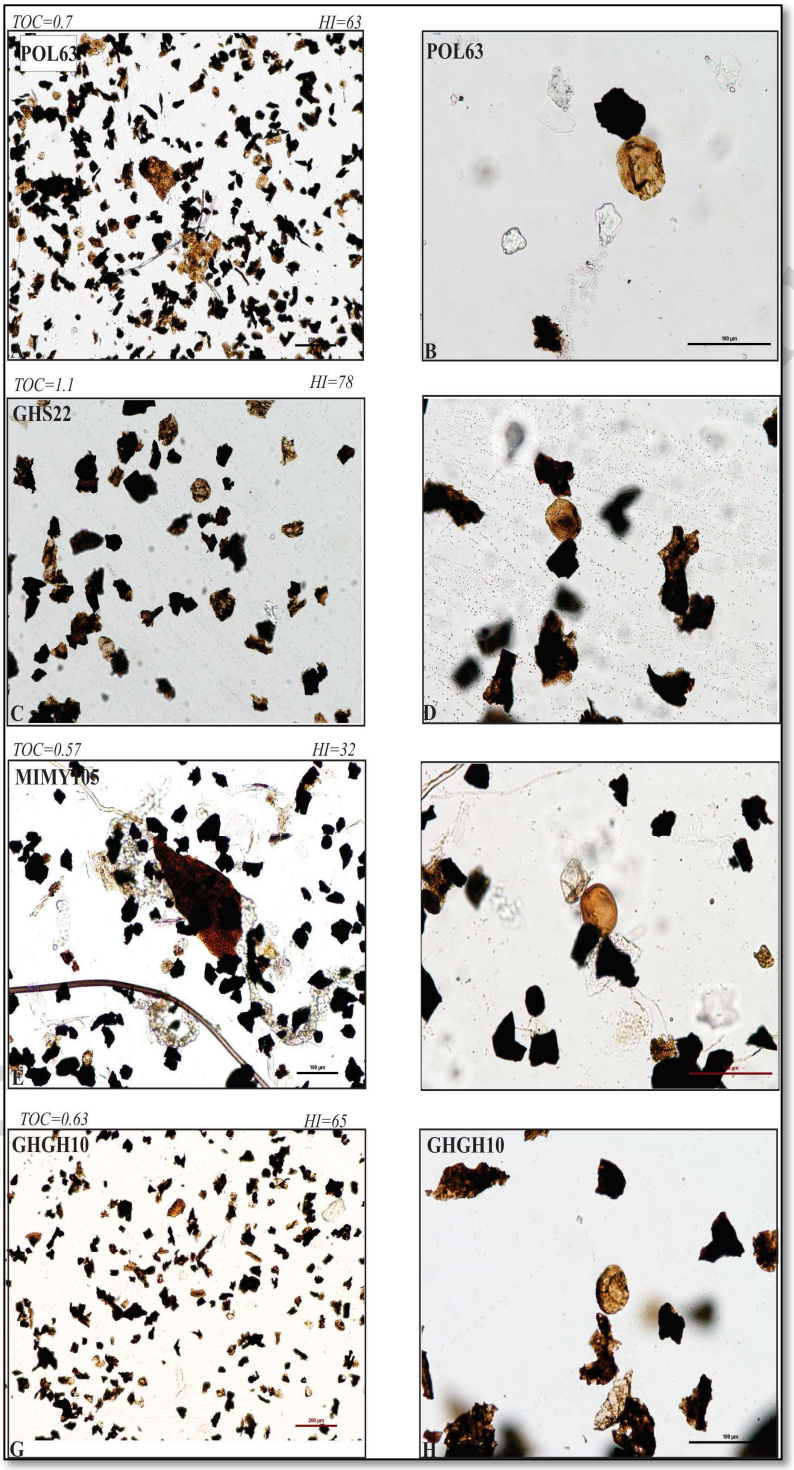

Figure 9. Microscopic images of organic matter (in the transmitted light). The left column shows an overview of the kerogen types, and the right column illustrates the brown spores with well to moderate accumulation from the same samples

As a result, the dark and black shaly facies from the Kashafrud Formation, specially from marine intervals, before thermal maturation, have been composed of Type II or II/III kerogen with moderate amounts of phytoclasts.

Thermal maturity assessment

Kerogen

T_{max} should be used with caution to assess thermal maturity especially in case of samples with low TOC and/or containing migrated HCs or contaminated with oil. Hence, in this study, only T_{max} values of those cutting samples that do not demonstrate oil contamination (S_1/TOC < 1.5) are accepted as interpretable T_{max} values. Regarding outcrop samples, T_{max} values of those samples possessing S_2 values higher than 0.1 mg HC/g rock and TOC greater than 0.2 wt% are recognized as valid T_{max} values.

The reliable T_{max} for the well samples which come from the upper part of the Kashafrud Formation, range from 441 to 470 °C (on average: 460 °C) and for the surface samples ranging from 325 to 603 °C (on average: 486 °C). T_{max} values < 400 °C ~~a~~are attributed to the presence migrated HCs.

Color of well-preserved sporomorphs ranges from pale brown to dark brown (Fig. 9) supports the T_{max} results. Reflectance of the indigenous vitrinite for the well samples ranges from 0.87 to 1.23%, indicating the samples are in oil generation window. For the surface samples, the range of vitrinite reflectance is larger, varying from 0.60 to 1.97%, indicating entrance into the oil window to end of wet gas-window. The VRo of two core samples is high with mean values 1.89 and 1.78%.

Bitumen

The carbon preference index (CPI) is an indicator for thermal maturition of bitumen. The CPI values higher and lower than 1 show thermally immature, while values near 1 are indicative of mature samples (Peters and Moldowan, 1993). The measured CPI values range from 0.91 to 1.03 for cutting samples and 0.86 to 1.04 for outcrop samples indicating high level of maturition, except for one sample from outcrop H, showing a low value of 0.56.

With increasing thermal maturition, Ts/Tm ratio (Ts = 18α(H)-trisnorneohopane; Tm = 17α(H)-trisnorhopane) increases (Peters and Moldowan, 1993; Waples, 1991). In general, most cutting and outcrop samples show a Ts/ Tm ratio higher than one (Table 3); hence, a high level of maturition for the samples can be deduced. Ts/Tm ratio is dependent on facies in addition to maturity. Carbonate source rocks indicate an uncommonly very low Ts/ Tm ratio (Moldowan et al., 1986; Shekarifard et al., 2019).

As maturition increases, the C_{31}-hopane 22S/(22S+22R) ratio rises from 0 to around 0.6 (equilibrium = 0.57–0.62) (Peters et al., 2005). Likewise, the C_{29}-Sterane 20S/(20S+20R) ratio goes up as thermal maturity increases, so that this ratio rises from 0 to nearly 0.5 (equilibrium = 0.52–0.55) (Seifert and Moldowan, 1986). The C_{31}-hopane 22S/(22S+22R) ratio achieved for the cutting (0.5 to 0.68) and outcrop samples (0.4 to 0.66) demonstrates the high thermal maturity for the samples. Furthermore, the measured C_{29}-Sterane 20S/(20S+20R) ratio for the cutting (0.28 to 0.58) and outcrop samples (0.27 to 0.65) confirms the high level of thermal maturity (Fig. 10c).

C_{23} homologs are dominant in the tricyclic terpenes in the extracted bitumen from the samples. The predominance of C_{23} tricyclic terpenes over C_{30} hopane show moderate to high maturition. These homologues (tricyclic terpenes) are resistant to maturition and increase with the increasing maturition level. The mentioned maturity-related parameters have been provided in Table 3.

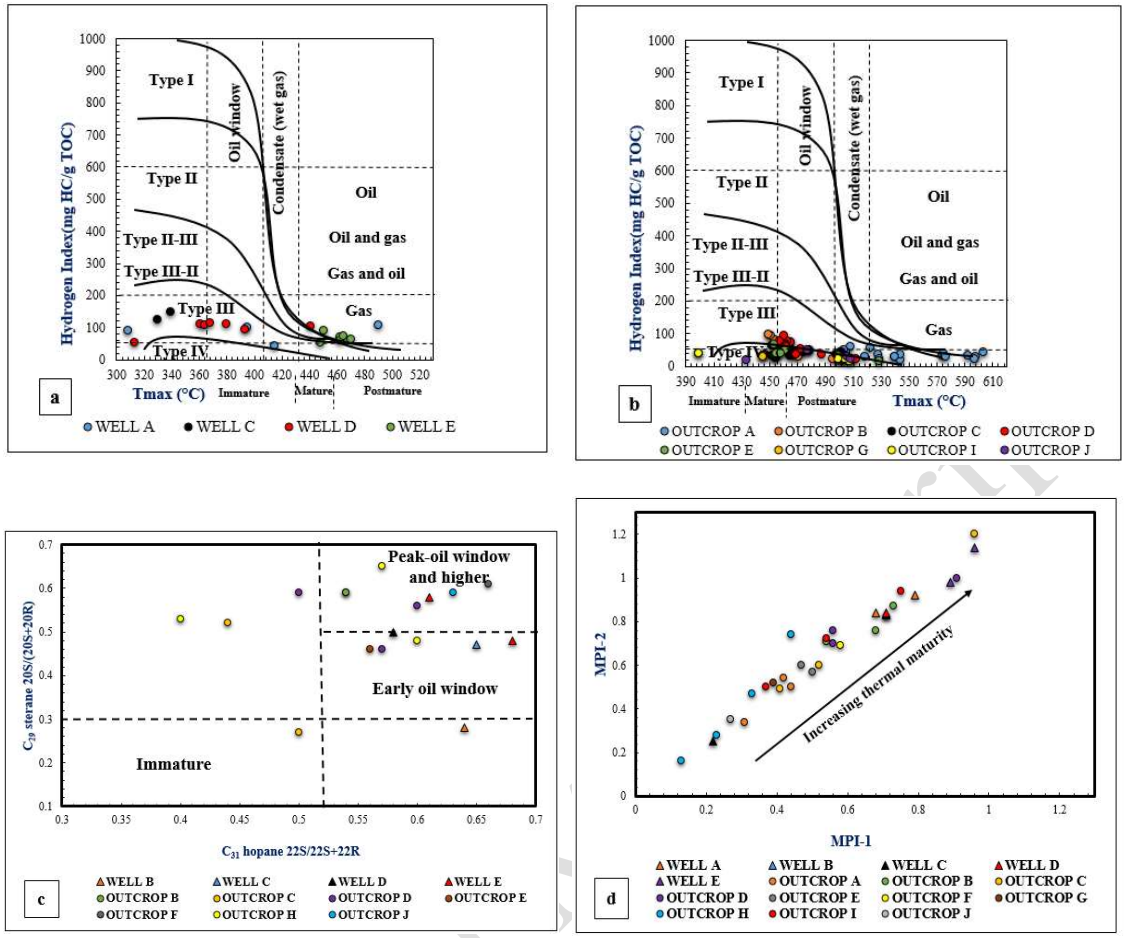

Figure 10. HI versus T_{max} indicating kerogen type and thermal maturity from well (a) and outcrop samples (b), plot of C_{29}-Sterane 20S/(20S+20R) versus C_{31}-hopane 22S/(22S+22R) (c) and MPI-1 versus MPI-2 (d) indicating thermal maturity level of well and outcrop samples

Methylphenanthrene Indices of MPI-1 and MPI-2 are widely used parameters in detecting maturition (Radke et al., 1982; Radke, 1988). These indexes show a positive correlation with VRo. MPI-1 can be normalized with VRo values (Radke & Welte, 1983). Generally, in the range of the oil window, there is a direct link between MPI-1 and VRo. In contrast, there is a negative correlation between these parameters at higher maturities (VRo > 1.35%) (Radke & Welte, 1983).

The MPI-1 value for the cutting samples is between 0.22 and 0.96, and for the outcrop samples ranges from 0.13 to 0.96. Hence, the cutting and outcrop samples are mature. Low values of MPI-1 in outcrops A, H, and J (0.44, 0.13, and 0.27, respectively) can be attributed to the severe impact of high maturition, leading to a reverse trend in thermal maturity level. The measured VRo values (Table 5) confirm it. Furthermore, the plot of MPI-1 versus MPI-2 (Fig. 10d) shows the maturition trend of the samples.

The MDBT (4-methyldibenzothiophene/1-methyldibenzothiophene) index is another proper maturity-related parameter suggested by Radke et al., 1986, based on the fact that 4-methyldibenzothiophene is more stable compared to 1-methyldibenzothiophene. However, this ratio is more useful at high levels of thermal maturity (e.g., light oil and condensate generation zone) (Dzou et al., 1995). It has been suggested that the 1-MDBT is stable across a wide range of maturities, while 4-MDBT increases with increasing thermal maturity. Correspondingly, $\frac{4-MDBT}{1-MDBT}$ ratio rises with increasing maturition (Dzou et al., 1995). The MDBT index ranging

from 1.71 to 8.69, and 2.7 to 12.45 for the cutting and outcrop samples, respectively (Table 5). Therefore, in consistent with other results, a moderate to high level of thermal maturity can be inferred from top to base of the Formation.

It should be mentioned that because the cutting samples predominately come from the upper 200 meters of the Kashafrud Formation and outcrops samples belong to entire of the Formation, this difference in recorded maturity and maturity-related parameters is normal and expected.

Origin of the bitumen

To investigate the origin of bitumen extracted from the samples, many molecular parameters from GC and GC-MS techniques were used.

According to Fig. 11a, the bitumen of the Kashafrud Formation is derived from different kerogen ranging from Type II, Type II-III, and Type III. However, majority of samples show Type II kerogen, deposited in a marine environment under anoxic to suboxic conditions (Didyk et al., 1978). Interestingly, the cutting samples show Type II kerogen, whereas majority of outcrop samples show the Type II-III and III (Fig. 11a). Samples from sections B and D show Type III kerogen. These results are consistent with sedimentology and facies analysis, indicating the upper part of the Formation were deposited in marine environment and lower parts are non-marine sediemts (Taheri et al., 2009).

Although for the cutting samples, the bitumen has been originated from marine algal but microscopic evidence confirms the presence of moderate amounts of phytoclasts. This represents the residual TOC recorded for the samples, is not totally linked to Type II kerogen and some parts of TOC belong to Type III-IV kerogen.

Generally, OM with marine origin demonstrate the sterane/hopane ratio values equal or higher than unity (Peters et al., 2005). All cutting and outcrop samples have the sterane/hopane ratio higher than 1 (1 to 3.59). Accordingly, a marine environment can be inferred for the Kashafrud Formation (Fig. 11c). Likewise, the majority of samples indicate the C_{26}/C_{25} tricyclic values lower than 1 (0.5 to 1.1), clarifying a marine origin (Zumberge, 1987).

Commonly, C_{27} regular steranes are indicative of marine phytoplankton, while C_{28} regular steranes are derived from lacustrine algae (Waples & Machihara, 1991). In the samples, C_{28} and C_{29} steranes have a lower frequency than C_{27} steranes. This clearly suggests a marine source for OM. The plot of the C_{27}/C_{29} ratio versus Pr/Ph ratio (Fig. 11c) suggests that the samples were deposited in an anoxic to suboxic marine depositional environment. Additionally, based on the plot of $C_{31}R/C_{30}$ hopane versus Pr/Ph, all samples demonstrate carbonate and marine shale origin (Fig. 11d).

In general, higher diasteranes values show terrigenous or clay-rich facies, whereas clay-poor facies, such as carbonates, commonly have low diasteranes (Mello et al., 1988; Peters et al., 2005). The C_{27} Dia/ (Dia+Reg) sterane can also be affected by thermal maturition. However, in this study, it appears that high values of this ratio for samples (0.37 to 0.75) show high ratio of clay to organic matter. Moreover, the ratio of C_{23}/ C_{24} tricyclic terpane can be used to investigate the source of bitumen. High values of this ratio demonstrate a marine carbonate source (Peters & Moldowan, 1993). However, this ratio also can be affected by maturity and increase as maturity rises. The very high values of C_{23}/ C_{24} tricyclic terpane for the cutting and outcrop samples (1.89 to 3.93) suggest the impact of thermal maturition rather than the depositional environment.

The ratio of Dibenzothiophene to Phenanthrene (DBT/Phen) is frequently employed to identify source rocks lithology and depositional environment. Commonly, values higher than 1 demonstrate carbonate and marly source rocks, while values lower than 1 imply shaly source rocks (Hughes et al., 1995). The samples show a DBT/Phen ratio lower than 1, hence a shaly lithology.

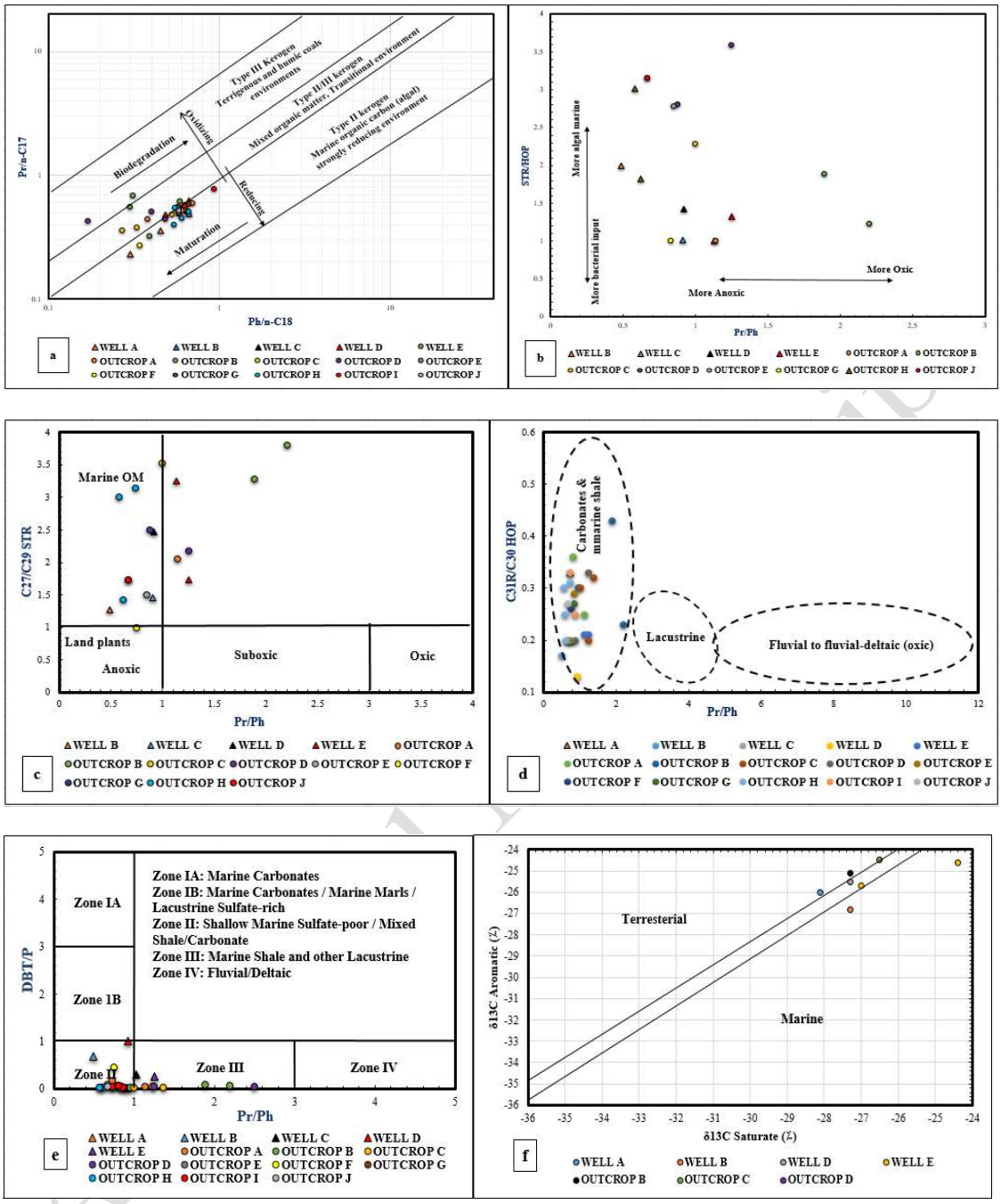

Figure 11. a: Plot of Pr/nC17 versus Ph/nC18 illustrating the depositional environment, kerogen type, and thermal maturity of OM, b: Steranes/Hopanes versus Pr/Ph indicating depositional environment, c: C_{27}/C_{29} versus Pr/Ph suggesting depositional environment, d: $C_{31}R/C_{30}$ Hopanes versus Pr/Ph typifying source and depositional setting, and d: DBT/P versus Pr/Ph showing depositional environment

Furthermore, the DBT/Phen versus Pr/Ph ratio is widely used to understand the depositional environment and lithology. As illustrated in Fig. 11e, all samples are located in zone II, implying a shallow marine sulfur-poor with a mixed shale and carbonate, in consistent with the calcimetry results. However, some samples show zone III, indicating marine shale depositional setting.

A canonical variable (CV) is characterized as the difference between the marine and

terrestrial equations used to identify the depositional setting. CV > 0.47 indicates terrestrial OM, whereas CV < 0.47 suggests marine OM (Sofer, 1984). The measured CV for the extracted bitumens of the Kashafrud Formation ranges from -2.07 to 1.72 (Table 7). Correspondingly, a mixed marine and terrestrial depositional environment can be inferred for the Kashafrud Formation in the studied area. Additionally, according to the plot of $\delta^{13}C$ Saturate (‰) versus. $\delta^{13}C$ Aromatic (‰) (Fig. 11f), the majority of samples demonstrate a mixed terrestrial and marine source (Fig. 11f).

Oil expulsion evidence

Free oil in the rock could consist of indigenously expelled HCs, migrated HCs, or contamination from oil-based mud or other well additives (El Diasty et al., 2018). Since water-base mud was used for drilling, there is no reason to suppose contamination by additives.

The ratio of S_1 to TOC discriminates between the indigenous HCs (i-HCs) and non-indigenous HCs (ni-HCs) in the source rock samples (Hunt, 1996). The ratio of $S_1 \times 100/TOC$ which is so-called migration index (MI) greater than 150 and production index (PI) (S_1/S_1+S_2) values greater than 0.3-0.4 are a sign of oil contamination by migrated HCs (Hunt, 1996). Furthermore, high S_1 values, anomalously low T_{max}, bimodal S_2 peak also are other evidence representing the samples contaminated by migrated HCs.

Figs. 12 a&b plot TOC versus S_1 to show the contaminated and non-contaminated cutting and outcrop samples, respectively. Although Fig 12a demonstrates that all analysed samples from well D non- contaminated, but individual parameters of based Rock-Eval data including very low T_{max} (313 to 393 °C) and high PI (0.29 to 0.46) show the occurrence of oil contamination in some samples. For well A and E, some samples contain i-HCs and some have ni-HCs. By contrast, all samples from wells B and C have oil contamination. For instance, in well B, the mean MI and PI values are 350 and 0.68, respectively. In this well, the mean S_1 (1.39 mg HC/g rock) values are more than twice the S_2 values (0.65 mg HC/g rock). The cross plot of MI versus depth for cutting samples (Fig. 12c) confirms the results obtained in Fig. 12a. Collectively, because the Kashafrud Formation is the oldest and main possible source rock in the area, it can be argued that organic facies from this Formation, in some regions (deep horizons in which the source rock is active), has even generated and expelled liquid petroleum. The generated liquid petroleum then migrated toward shallower depths.

Oil staining is further supported by organic petrography evidence. Many cutting samples show low to medium bitumen staining. In some cases, bitumen staining in this well corroborates the results obtained by Rock-Eval pyrolysis and demonstrates that studied samples have been affected by migrated HCs. The presence of vitrinite maceral is common, and oil stains were observed on large vitrinite particles (Fig. 13). Under UV light, orange AOM was commonly present. As shown in Fig. 13, the highly stained particles have been surrounded by brown bitumen. Particles associated with framboidal pyrites (right) show more intense stains. Accordingly, bitumen staining is observed as cavity-like fluorescence. It should be noted that vitrinite particles that have not been affected by bitumen staining do not show fluorescence.

Although based on the Rock-Eval data (S_1/TOC ratio), the surface samples due to weathering do not show the ni-HCs, but based on organic petrography bitumen staining observed in many analysed outcrop samples. Also, other outcrop micrographs illustrate a low to moderate staining (Figs 13 b & d h). In Figure 103b, residual oil stains can be seen on fine-grained vitrinite particles. It should be noted that staining can reduce vitrinite reflectance (VRo) values.

Geochemical comparison of the i-HCs and ni-HCs (bitumen)

By comparing the molecular geochemical properties of the i-HCs and ni-HCs, the genetic

relationship of these HCs can be determined. Because in some cases, ni-HCs may have entered into the source rock from other formations and are entirely opposed to the i-HC resulting from insitu kerogen maturation. If i-HCs and ni-HCs within a geological sequence have similar geochemical properties, it is natural and reasonable to assume that these i-HCs and ni-HCs have the same origin, although ni-HCs have been generated from the same Formation and at different intervals. In this study, although bitumen samples have undergone high thermal maturition, we attempt to compare their genetic relationship.

For this purpose, based on the Rock-Eval pyrolysis data five samples were selected from the wells B, C, D, and E which show indigenous and non-indigenous HCs; three samples with ni-HCs and two samples with i-HCs (Table 6).

For these investigated samples, GC data, including the ratios of Pr/Ph, CPI, Pr/nC_{17}, and Ph/nC_{18} (Table 6), confirm that these two types of bitumen (HCs) have more or less the same properties. Therefore, it is logic to assume that these two types of bitumen (HCs) with similar thermal maturity, have generated from the same organic facies with a same origin. However, there is a significant difference in biomarker indicators of DBT/Phen, and C_{29}/C_{30} hopane.

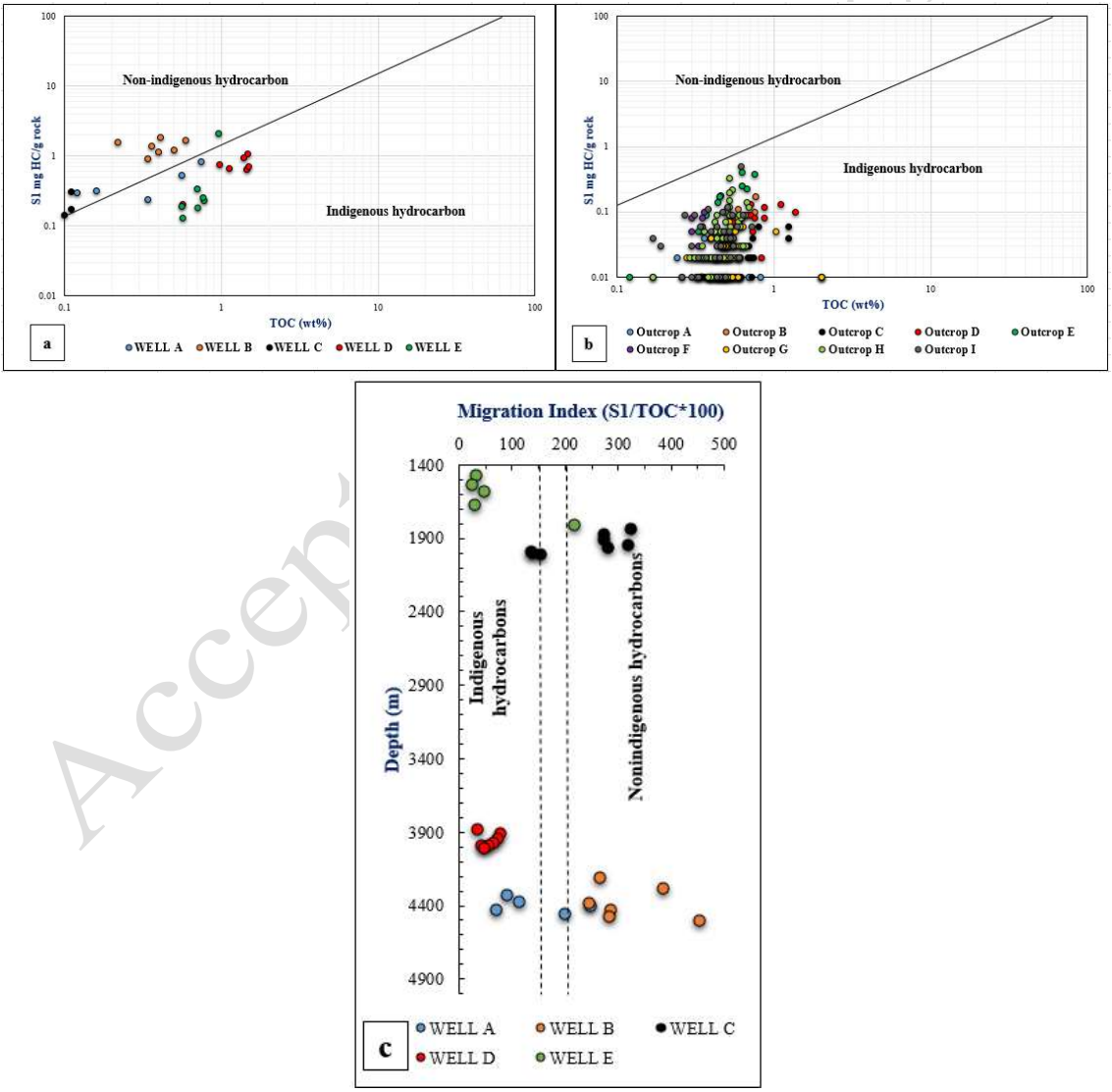

Figure 12. Plots of S1 versus TOC for well (a) and outcrop samples (b) and migration index versus depth (c) for cutting samples

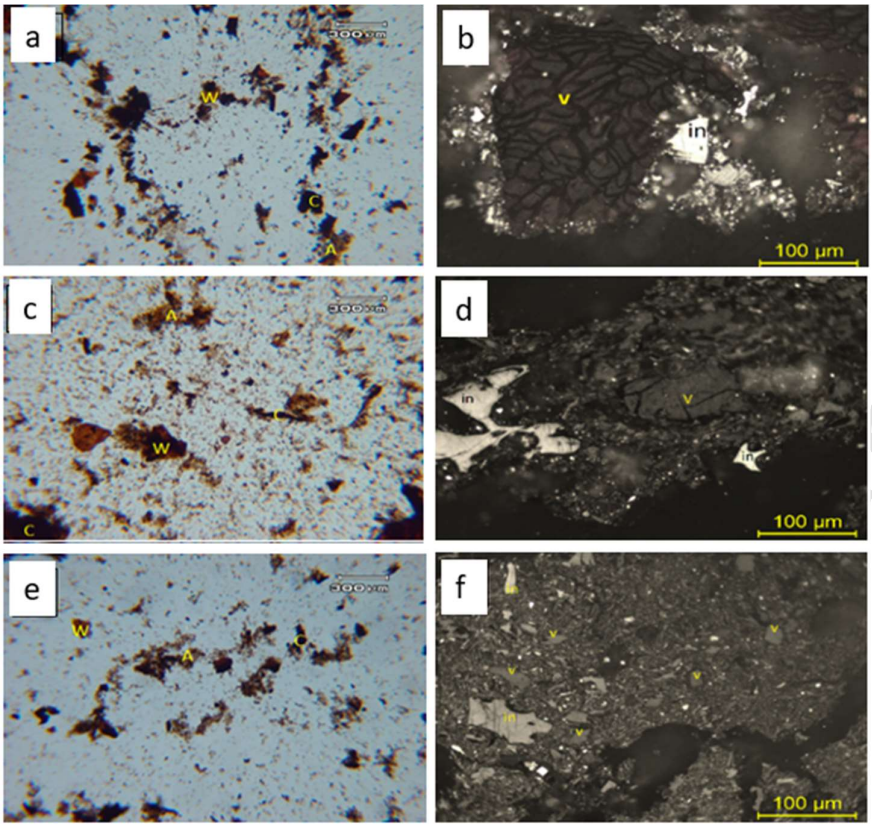

Figure 13. Microscopic images (under transmitted light) of dispersed organic matter in the shay sediments from the Kashafrud Formation (a, c, e). Microscopic images (under reflected light) of organic matter from the same samples indicating the evidence of oil staining (b, d, f). A (Amorphous organic matter), W (Woody particles), C (Coaly particles), V (Vitrinite), In (inertinite)

In the studied wells, the mean DBT/Phen ratio for samples with i-HCs is about 0.13, whereas for samples with ni-HCs is 0.96. For these samples, the mean value of C_{29}/C_{30} hopane for the i-HCs and ni-HCs is 0.98 and 1.42, respectively. These biomarker parameters clearly indicates that the ni-HCs have been derived from the organic facies with more properties of carbonate source rocks, deposited under more anoxic conditions. This result is consistent with petrography evidence and calcimetry results, indicating the occurrence of mixed siliciclastic-carbonate facies in the Kashafrud Formation. These biomarker ratios also clarifies that the ni-HCs are a little more sulfurous, in compared with the i-HCs. The carbonate facies have been proven to be more prone to generating sulfuric HCs.

The GC-MS results indicate that the i-HCs have been derived from more pure shaly facies, whereas the ni-HCs have been generated from are more carbonate shaly facies. As a results, it seems although shaly facies from the Formation, especially for sample with low TOC, has been acted as a gas-prone source rock, but the carbonate-rich facies, especially for samples with higher TOC, have played an effective source rock to generate and expel liquid (oil) petroleum.

These results with organic petrography evidence clearly confirm that some parts of the source rocks from the Formation have generated and expelled liquid petroleum. Generally, carbonate facies generate petroleum at lower TOC values than siliciclastic facies. Also, petroleum expulsion from carbonate source rocks is easier than from siliciclastic facies (Hunt, 1996).

Conclusion

The results indicate that the mean residual TOC from the shaly facies of the Middle Jurassic

Kashafrud Formation is 0.56 wt% and 0.4 wt% for the wells and outcrop samples, respectively.

Kashafrud Formation is thermally mature to over-mature. The Formation has acted as an effective source rock and still has some potential to generate gas and condensate. The Formation in the subsurface (wells) is still an active effective source rocks, but in the outcrops it is inactive. Before thermal maturation, source rocks from the Formation, have had high potential to generate gas and oil. The kerogen in the shaly units is characterized by dominance of amorphous OM (AOM) with marine phytoplankton/algal origin and moderate to high amounts of higher land plant debris. Biomarker analyses reveal the bitumen extracted (indigenous HCs) from the upper part of the Formation has derived mainly from Type II kerogen, whereas the lower part of the Formation is originated from a mixture of Type II, II-III and III kerogen. This evidence is consistent with sedimentology analyses that show the upper parts of the Formation were deposited in marine environments, whereas the lower parts indicate the more characters of non-marine deposits. The non-indigenous HCs (ni-HCs) have been generated from mixed siliciclastic-carbonate facies. As a results, it seems although shaly facies, especially for sample with low TOC, a gas-prone source rock, but the more carbonate facies, especially for samples with higher TOC, generated and expelled oil.

Conflicts of interest

The authord declare that they have no conflicts of interest

Authors' contributions

All authors contributed to the design and implementation of the research, to the analysis of the results and to the writing of the manuscript.

Appendix 1

Abbreviation of peak assignments for alkane petroleums derived from gas chromatography of the saturate fractions in m/z 191 (I) and m/z 217(II).

(I) Peak No		
Tm	17α(H),22,29,30-trisnorhopane	Tm
29	17α,21β(H)-nor-hopane	C29 hop
30	17α,21β(H)-hopane	Hopane
30M	17 β,21α (H)-Moretane	C30Mor
29M	17β (H),2lα (H)-30-norhopane (normoretane)	Normoretane
31S	17α,21β(H)-homohopane (22S)	C31(22S)
31R	17α,21β(H)-homohopane (22R)	C31(22R)
32S	17α,21β(H)-homohopane (22S)	C32(22S)
32R	17α,21β(H)-homohopane (22R)	C32(22R)
33S	17α,21β(H)-homohopane (22S)	C33(22S)
33R	17α,21β(H)-homohopane (22R)	C33(22R)
34S	17α,21β(H)-homohopane (22S)	C34(22S)
34R	17α,21β(H)-homohopane (22R)	C34(22R)
35S	17α,21β(H)-homohopane (22S)	C35(22S)
35R	17α,21β(H)-homohopane (22R)	C35(22R)
(II) Peak No.		
a	13β,17α(H)-diasteranes 20S	Diasteranes
b	13β,17α(H)-diasteranes 20R	Diasteranes
c	13α,17β(H)-diasteranes 20S	Diasteranes
d	13α,17β(H)-diasteranes 20R	Diasteranes
e	5α,14α(H), 17α(H)-steranes 20S	ααα20S
f	5α,14β(H), 17β(H)-steranes 20R	αββ20R
g	5α,14β(H), 17β(H)-steranes 20S	αββ20S
h	5α,14α(H), 17α(H)-steranes 20R	ααα20R

References

Afshar-Harb, A., 1979. The Stratigraphy, Tectonics and Petroleum Geology of the Kopet Dagh Region, Northern Iran, 219 p.

Afshar-Harb, A., 1969. History of oil exploration and brief description of the geology of the Sarakhs area and the anticline of Khangiran. Bull. Iran. Pet. Inst. 37: 86-94.

Aghababaei, A., Rahimi, B., Farzin Ghaemi, F., Moussavi-Harami, R., Motamedi, H., Gholami Zadeh, P., 2024. Tectonostratigraphy of the Upper Jurassic-Lower Cretaceous siliciclastic (Shurijeh Formation) in the eastern Kopeh Dagh fold and thrust belt, Iran. Marine and Petroleum Geology. 164 p.

Brunet, M., Korotaev, M., Ershov, A., Nikishin, A., 2003. The South Caspian Basin: a review of its evolution from subsidence modelling. Sediment. Geol. 156(1-4): 119-148.

Coplen, T., 1995. Reporting of stable hydrogen, carbon, and oxygen isotopic abundances-(Technical report). Geothermics 24(5): 708-712.

Didyk, B.M., Simoneit, B.R.T., Brassell, S.C. t, Eglinton, G., 1978. Organic geochemical indicators of palaeoenvironmental conditions of sedimentation. Nature 272, 216.

Dzou, L.I., Noble, R.A., Senftle, J., 1995. Maturation effects on absolute biomarker concentration in a suite of coals and associated vitrinite concentrates. Org. Geochem. 23(7): 681-697.

El Diasty, W.S., El Beialy, S.Y., Peters, K.E., Batten, D.J., Al-Beyati, F.M., Mahdi, A.Q., Haseeb, M.T., 2018. Organic geochemistry of the Middle-Upper Jurassic Naokelekan Formation in the Ajil and Balad oil fields, northern Iraq. J. Pet. Sci. Eng. 166: 350-362.

Frizon de Lamotte, D., Raulin, C., Mouchot, N., Wrobel-Daveau, J., Blanpied, C., Ringenbach, J., 2011. The southernmost margin of the Tethys realm during the Mesozoic and Cenozoic: Initial geometry and timing of the inversion processes. Tectonics 30 : Issue 3.

Garzanti, E., Gaetani, M., 2002. Unroofing history of late Paleozoic magmatic arcs within the "Turan plate"(Tuarkyr, Turkmenistan). Sediment. Geol. 151(1-2): 67-87.

Green, O., 2001. Preparation of amber specimens containing fossils, in: A Manual of Practical Laboratory and Field Techniques in Palaeobiology. Springer, Dordrecht, 538 pages: 234-241.

Hughes, W.B., Holba, A.G., Dzou, L.I.P., 1995. The ratios of dibenzothiophene to phenanthrene and pristane to phytane as indicators of depositional environment and lithology of petroleum source rocks. Geochim. Cosmochim. Acta 59: 3581-3598.

Hunt, J.M., 1996. Petroleum geochemistry and geology. WH Freeman New York, 332 pages.

Jarvie, D., Morelos, A., Han, Z., 2001. Detection of pay zones and pay quality, Gulf of Mexico: Application of geochemical techniques. AAPG, 51: 151-160.

Javanbakht, M., Wanas, H., Jafarian, A., Shahsavan, N., Sahraeyan, M., 2018. Carbonate diagenesis in the Barremian-Aptian Tirgan Formation (Kopet-Dagh Basin, NE Iran): petrographic, geochemical and reservoir quality constraints. J. African Earth Sci. 144: 122-135.

Jones, R., 1984. Comparison of carbonate and shale source rocks No Title, in: Petroleum Geochemistry and Source Rock Potential of Carbonate Rocks. AAPG Special Volumes, pp. 163-180.

Karamati, M., Tavallai, M., Angaji, M. Memariani, M., 2000. Hydrocarbon potential and migration system of Kashafroud Formation, in Kopet Dagh sedimentary basin, NE Iran. 16th World Petroleum Congress, Calgary, Canada.

Kavoosi, M., Lasemi, Y., Sherkati, S., Moussavi-Harami, R., 2009. Facies analysis and depositional sequences of the Upper Jurassic Mozduran Formation, a carbonate reservoir in the Kopet Dagh Basin, NE Iran. J. Pet. Geol. 32(3): 235-259.

Kazmin, V., Tikhonova, N., 2005. Early Mesozoic marginal seas in Black Sea-Caucasus region: Paleotectonic reconstructions. Geotectonics 39(5): 349-363.

Lasemi, Y., 1995. Platform carbonates of the Upper Jurassic Mozduran formation in the Kopet Dagh Basin, NE Iran-facies, palaeoenvironments and sequences. Sediment. Geol. 99(3-4): 151-164.

Magoon, L., Dow, W.., 1994. The petroleum system. In: Magoon, L.B., Dow, W.G. (Eds.), The Petroleum System: From Source to Trap. Am. Assoc. Pet. Geol. Mem. 60: 3-24.

Mello, M.R., Telnaes, N., Gaglianone, P.C., Chicarelli, M.I., Brassell, S.C., Maxwell, J.R., 1988. Organic geochemical characterisation of depositional palaeoenvironments of source rocks and oils in Brazilian marginal basins, in: Organic Geochemistry In Petroleum Exploration. Elsevier, pp. 31-45.

Moldowan, J.M., Sundararaman, P., Schoell, M., 1986. Sensitivity of biomarker properties to depositional environment and/or source input in the Lower Toarcian of SW-Germany. Org. Geochem. 10: 915-926.
Moshirfar, Y., Mahdavi, M., Ghasemi-Nejad, E., Ashouri, A., 2015. Eocene climatic events recorded in dinoflagellate cyst assemblages from the Koppeh-Dagh Basin, NE Iran; a statistical approach. Arab. J. Geosci. 8(2): 867-876.
Moussavi-Harami, R., 1986. Neocomian (Lower Cretaceous) continental sedimentation in eastern Kopet-Dagh in NE Iran, in: 12th International Sedimentological Congress. Canberra.
Moussavi-Harami, R., Brenner, R., 1992. Geohistory analysis and petroleum reservoir characteristics of Lower Cretaceous (Neocomian) sandstones, eastern Kopet-Dagh Basin, northeastern Iran. American Association Of Petroleum Geologists. Bull. 76(8): 1200–1208.
Peters, K.E., 1986. Guidelines for evaluating petroleum source rock using programmed pyrolysis. Am. Assoc. Pet. Geol. Bull. 70: 318-329.
Peters, K.E. Cassa, M.C., 1994. Applied Source Rock Geochemistry. In The Petroleum System-From Source To Trap, Magoon, B and Wallace, G.Dow (Eds), American Association Of Petroleum Geologists Memoir, 60: 93-117.
Peters, K.E., Moldowan, J.M., 1993. The biomarker guide (V.1) : interpreting molecular fossils in petroleum and ancient sediments,. Prentice Hall, New Jersey, 352 p.
Peters, K.E., Walters, C.C., and Moldowan, J.., 2005. The Biomarker Guide: Biomarkers and isotopes in petroleum systems and Earth history, 1132 p.
Poursoltani, M., Gibling, M., 2011. Composition, porosity, and reservoir potential of the Middle Jurassic Kashafrud Formation, northeast Iran. Mar. Pet. Geol. 28(5): 1094-1110.
Poursoltani, M., Moussavi-Harami, R., Gibling, M., 2007. Jurassic deep-water fans in the Neo-Tethys Ocean: the Kashafrud Formation of the Kopet-Dagh basin, Iran. Sediment. Geol. 198(1–2): 53-74.
Radke, M., 1988. Application of aromatic compounds as maturity indicators in source rocks and crude oils. Mar. Pet. Geol. 5: 224-236.
Radke, M., Welte, D., 1983. The methylphenanthrene index (MPI): a maturity parameter based on aromatic hydrocarbons. Advances in Organic Geochemistry, 1983, 1981: 504-512.
Radke, M., Welte, D., Willsch, H., 1986. Maturity parameters based on aromatic hydrocarbons: Influence of the organic matter type. Org. Geochem. 10(1-3): 51-63.
Radke, M., Welte, D.H., Willsch, H., 1982. Geochemical study on a well in the Western Canada Basin: relation of the aromatic distribution pattern to maturity of organic matter. Geochim. Cosmochim. Acta 46: 1-10.
Raisossadat, S., Moussavi-Harami, R., 1993. Stratigraphy and Biozonation of Sarcheshmeh and Sanganeh Forma tions in Eastern Kopet Dagh Basin. Geol. Surv. Iran. Geosci. 2(7): 58.
Robert, A., Letouzey, J., Kavoosi, M.., Sherkati, S., Müller, C., Vergés, J., Aghababaei, A., 2014. Structural evolution of the Koppeh Dagh fold-and-thrust belt (NE Iran) and interactions with the South Caspian Sea Basin and Amu Darya Basin. Mar. Pet. Geol. 57: 68-87.
Shahidi, A., 2008. Evolution tectonique du Nord de l'Iran (Alborz et Kopet-Dagh) depuis le Mésozoïque (Doctoral dissertation, Paris 6).
Sharafi, M., Ashuri, M., Mahboubi, A., Moussavi-Harami, R., 2012. Stratigraphic application of Thalassinoides ichnofabric in delineating sequence stratigraphic surfaces (Mid-Cretaceous), Kopet-Dagh Basin, northeastern Iran. Palaeoworld, 21(3-4): 202-216.
Sofer, Z., 1984. Stable carbon isotope compositions of crude oils: application to source depositional environments and petroleum alteration. Am. Assoc. Pet. Geol. Bull. 68(1): 31-49.
Sofer, Z., 1980. Preparation of carbon dioxide for stable carbon isotope analysis of petroleum fractions. Anal. Chem. 52(8): 1389-1391.
Taheri, J., Fürsich, F.T., Wilmsen, M., 2009. Stratigraphy, depositional environments and geodynamic significance of the Upper Bajocian Bathonian Kashafrud Formation, NE Iran. In: South Caspian to Central Iran Basins, M.F. Brunet, M. Wilmsen, J.W. Granath (eds). The Geological Society, London, Special Publications 312: 205-218.
Tissot, B.P., Welte, D.H., 1978. Petroleum Formation and Occurrence: A New Approach to Oil and Gas Exploration. Springer-Verlag, New York 538 p.
Ulmishek, G.F., 2004. Petroleum geology and resources of the Amu–Darya Basin, Turkmenistan, Uzbekistan, Afghanistan, and Iran. U.S. Geol. Surv. Bull. 2201 (4): 32 p.

Waples, D.W., 1991. Biomarkers for geologists-a practical guide to the application of steranes and triterpanes in petroleum geology. Chap., 5-10.
Waples, D.W., Machihara, T., 1991. Biomarkers for geologists–a practical guide to the application of steranes and triterpanes. In: Petroleum Geology, American Association of Petroleum Geologists Methods in Exploration, Series, 9: 20-91.
Zaheri, S., 2022. Organic Geochemistry and Hydrocarbon Generation Modelling of the Kashafrud Formation in East of Mazdavand (South East of Mashhad), Master Thesis, Shahid Beheshti University.
Zumberge, J.E., 1987. Terpenoid biomarker distributions in low maturity crude oils. Org. Geochem. 11(6): 479-496.